frontiers | Frontiers in Materials

TYPE Original Research
PUBLISHED 03 April 2025
DOI 10.3389/fmats.2025.1576078



OPEN ACCESS

EDITED BY
Antonios Kanellopoulos,
University of Hertfordshire, United Kingdom

REVIEWED BY
Salvatore Verre,
University of eCampus, Italy
Chuanqing Fu,
Zhejiang University of Technology, China

*CORRESPONDENCE
Wangwen Sun,
2024021081@chd.edu.cn
Lauren Y. Gómez-Zamorano,
lauren.gomezzm@uanl.edu.mx

RECEIVED 13 February 2025
ACCEPTED 24 March 2025
PUBLISHED 03 April 2025

CITATION
Ye W, Feng T, Sun W and Gómez-Zamorano LY (2025) Enhancing steel slag cement mortar performance under low-temperature curing through alkali activation: mechanisms and implications. *Front. Mater.* 12:1576078. doi: 10.3389/fmats.2025.1576078



# Enhancing steel slag cement mortar performance under low-temperature curing through alkali activation: mechanisms and implications

Wei Ye[1], Tengteng Feng[2], Wangwen Sun[2]* and Lauren Y. Gómez-Zamorano[3]*

[1]Xinjiang Jiaotou Construction Management Co., Ltd., Urumchi, China, [2]School of Highway, Chang'an University, Xi'an, China, [3]Programa Doctoral en Ingeniería de Materiales, Facultad de Ingeniería Mecánica y Eléctrica, Universidad Autónoma de Nuevo León, San Nicolás de los Garza, Nuevo León, Mexico

The effective utilization of steel slag waste offers a sustainable approach to advancing construction materials, particularly in cold regions. This study investigates the influence of alkaline activators and low-temperature curing (10°C) on the performance of steel slag cement mortar. The setting time of mixed slurry with varying steel slag powder content was analyzed, along with the effects of different activators and water glass modulus on compressive strength. Advanced characterization techniques, including thermogravimetric analysis (TGA), X-ray diffraction (XRD), and scanning electron microscopy (SEM), were employed to examine the hydration products and microstructural evolution of optimally activated samples. The results indicate that a $Na_2O$ content of 4% significantly enhances the compressive strength of steel slag cement mortar. The composite activator (containing water glass and NaOH) exhibited superior performance compared to neat NaOH, increasing the strength. Activated samples demonstrated increased early hydration products, as evidenced by intensified $Ca(OH)_2$ diffraction peaks. The activators facilitated calcium ion dissolution, reduced the activation energy of cementitious materials, and accelerated hydration kinetics, leading to the enhanced formation of hydration products. Microstructural analysis revealed that the activators disrupted the vitreous network structure of the steel slag powder, promoting more complete hydration and the formation of dense C-S-H gels and $Ca(OH)_2$. This densification reduced porosity and significantly improved the mechanical properties of the cement matrix. These findings highlight the potential of alkaline-activated steel slag cement mortar as a sustainable and high-performance material for construction applications in cold climates.

KEYWORDS

**low temperature curing, alkaline activator, steel slag cement, microstructure, mechanisms**

# 1 Introduction

The global steelmaking industry generates significant amounts of byproducts, with steel slag alone representing around 15% of the total global crude steel production each year (Bilim and Atiş, 2012; Guo et al., 2018b). Steel slag is primarily composed of calcium silicates, aluminosilicates, the RO phase (a CaO-FeO-MgO-MnO solid solution), and forsterite, making it a potentially valuable resource for construction applications due to its cementitious properties (Xiong et al., 2022; Liu et al., 2020; Monshi and Asgarani, 1999). These properties suggest its utility as a supplementary cementitious material (SCM) in cement and concrete production, offering significant environmental and economic benefits. Despite its potential, the effective utilization of steel slag remains critically low. For instance, in China, an estimated 100 million tons of steel slag are generated annually, yet only 22% is effectively recycled. Utilization rates are even lower in many other parts of the world, reflecting a widespread failure to capitalize on this abundant resource (Yi et al., 2012; Li et al., 2011; Monshi and Asgarani, 1999; Kua, 2015; Xue et al., 2006; Qasrawi et al., 2009).

The underutilization of steel slag presents significant environmental challenges. Vast quantities of slag are often stockpiled or landfilled, occupying extensive land areas and causing serious environmental risks. These include leaching of heavy metals and alkaline substances into soil and water systems, which can lead to contamination and degradation of local ecosystems (Guo et al., 2018a). Verre (2021) highlighted the significant impact of aggressive environments, particularly alkaline conditions, on the durability and performance of cement-based composites. These findings emphasize the degradation mechanisms induced by alkalis and their critical implications for the design and application of cement-based materials. Furthermore, the accumulation of steel slag contributes to the growing global problem of industrial waste management, highlighting the urgency of developing sustainable and efficient recycling strategies to mitigate these issues.

In addition to addressing waste management challenges, the effective recycling of steel slag aligns with global efforts to reduce the environmental footprint of construction materials. By partially substituting traditional cementitious materials with steel slag, it is possible to reduce the demand for clinker, the production of which is a major contributor to $CO_2$ emissions in the cement industry. Moreover, the valorization of steel slag can contribute to a circular economy, transforming what is currently considered industrial waste into a valuable resource for infrastructure development. Such efforts are particularly important in the context of global urbanization and the increasing demand for sustainable construction materials (Bilim and Atiş, 2012; Guo et al., 2018a).

Incorporating steel slag into cement-based materials as a supplementary cementitious material (SCM) offers a promising solution for reducing environmental impacts while improving resource efficiency in the construction sector. By replacing traditional cementitious materials, steel slag can contribute to consumption reduction, energy conservation, and significant $CO_2$ emission reductions in the cement industry (Parron-Rubio et al., 2018; Shen et al., 2020; Miah et al., 2020). However, its application is hindered by the high content of inert components, such as $Fe_3O_4$ and the RO phase, which negatively affect early hydration processes, resulting in reduced early strength of cement and concrete (Zhang et al., 2021; Zhuang and Wang, 2021; Liu et al., 2021). To enhance the reactivity of steel slag and mitigate its performance limitations, several activation methods have been explored. These include mechanical, thermal, and chemical activation techniques, each with distinct advantages and limitations. Mechanical activation, which involves reducing the size of steel slag mineral crystals and dislocating their crystal lattices, has proven effective. However, achieving a specific surface area beyond 500 $m^2$/kg often results in increased energy consumption and costs, reducing its feasibility (Zhang et al., 2021). Thermal activation, on the other hand, effectively breaks Si-O and Al-O bonds, depolymerizing the glassy structure of steel slag, but it is impractical for on-site concrete preparation due to the high temperatures required. Consequently, chemical activation has emerged as a practical and efficient alternative.

Chemical activators, particularly sodium-based compounds such as sodium aluminate ($NaAlO_2$), sodium sulfate ($Na_2SO_4$), and sodium silicate ($Na_2SiO_3$), have shown significant potential in enhancing the early hydration characteristics of steel slag cement (Zhang et al., 2021). Among these, sodium silicate ($Na_2SiO_3$) has been particularly effective due to its ability to accelerate hydration reactions, promote the dissolution of calcium ions, and increase the formation of calcium-silicate-hydrate (C-S-H) gels, which are crucial for mechanical strength development. Studies have reinforced this effectiveness; Singh and Vashistha (2021) demonstrated that $Na_2SiO_3$ significantly enhances early hydration reactions and boosts the content of C-S-H gel in hydration products. Similarly, Atiş et al. (2009) compared various activators, including $Na_2SiO_3$, NaOH, and $Na_2CO_3$, and concluded that sodium silicate provides the most effective activation, enabling steel slag to achieve sufficient early strength and setting times comparable to traditional cement clinker. Furthermore, Bilim and Atiş (2012) observed that increasing the sodium content in liquid $Na_2SiO_3$ correlates with improved compressive strength and mechanical properties of steel slag cement, underscoring its potential as a key chemical activator. Despite these advancements, challenges persist, particularly under low-temperature curing conditions. The hydration process of steel slag cement is significantly slowed at low temperatures, which reduces the rate of strength development and impacts the final mechanical properties (Li et al., 2024; Dai et al., 2021; Liu et al., 2015). This limitation arises from the reduced kinetics of hydration reactions and the incomplete formation of hydration products under such conditions. Alkaline activators, including sodium silicate and sodium hydroxide (NaOH), have been found to promote hydration reactions by reducing activation energy and enhancing the dissolution of reactive phases, offering a promising strategy to mitigate the effects of low temperatures. However, the microstructural and mechanical impacts of alkaline activators on steel slag cement paste under low-temperature curing conditions remain underexplored. Existing studies primarily focus on ambient or elevated temperature conditions, leaving a critical gap in understanding the behavior and performance of steel slag cement mixtures in colder environments. Given the growing interest in utilizing industrial by-products in sustainable construction, addressing this knowledge gap is essential. Incorporating alkaline activators into steel slag cement mixtures offers the potential to significantly enhance both physical and mechanical properties under low-temperature curing. Such approaches could lead to more

widespread adoption of steel slag in construction applications, particularly in regions with cold climates. Furthermore, this strategy aligns with broader goals of sustainable development by increasing the utilization of steel slag, reducing industrial waste, and minimizing the environmental footprint of construction materials.

Following form that, the main objective of this study was to incorporate an alkaline solution, using NaOH and $Na_2SiO_3$ as activators, to enhance the reactivity of steel slag during the hydration process under constant low-temperature curing conditions. The research (Figure 1) evaluated the effects of NaOH incorporation and varying its content on the compressive strength of steel slag cement mortar. Additionally, the influence of $Na_2O$ content and water glass modulus in a combined activation approach was investigated to determine their impact on mechanical performance. To further understand these effects, microstructural characterization of the cement paste materials containing alkaline activators was conducted using X-ray diffraction (XRD), thermogravimetric analysis (TGA), and scanning electron microscopy (SEM). These techniques provided insights into hydration products and morphological changes in the material. The findings from this research highlight the potential of alkaline activators to significantly strengthen steel slag cement mortar under low-temperature conditions. Furthermore, the study underscores the broader implications for increasing the utilization of steel slag powder in cold regions, reducing industrial waste pollution, and promoting efficient resource recycling within the construction industry.

# 2 Materials and methods

## 2.1 Raw materials

The steel slag powder used in this study was sourced from Xinjiang Hegang Steel Co., Ltd. After initial processing, the material was sieved to ensure uniformity, and only steel slag powder with a particle size of less than 75 μm was selected for experimentation. This fine particle size ensures better reactivity and consistency in the hydration process. The chemical composition of the steel slag, represented by its oxide content, is presented in Table 1, while the mineral composition, determined *via* X-ray diffraction (XRD), is shown in Figure 2. The steel slag mainly consists of calcium silicates, aluminosilicates, and the RO phase (CaO-FeO-MgO-MnO solid solution), which contribute to the cementitious properties. The particle size distribution of the steel slag powder, compared to ordinary Portland cement, is illustrated in Figure 3. The steel slag powder shows a relatively fine particle size distribution, which facilitates packing density and potential reactivity in cementitious systems. The ordinary Portland cement (OPC) used in the experiments was P.O.42.5 grade cement, according to the Chinese standard GB 175-2007 (Standardization Administration of China, 2007). This type of OPC is widely used in construction applications and was chosen for its compatibility with steel slag in blended systems. The chemical composition analyzed consisted mainly of consists of CaO, $SiO_2$, $Al_2O_3$, and $Fe_2O_3$, which are critical for hydration and strength development (see Table 1). The chemical activators employed in this study were sodium hydroxide (NaOH) pellets with a purity of 96% and a commercial water glass solution, which is an aqueous sodium silicate solution. The sodium hydroxide was used to prepare alkaline solutions, while the water glass solution, characterized by its $SiO_2/Na_2O$ ratio (modulus), served as a source of silicate ions to enhance the hydration reaction. The selection of these activators was based on their ability to promote the hydration of steel slag and improve the mechanical properties of blended cementitious materials. The combination of steel slag powder, ordinary Portland cement, and chemical activators in this study was designed to investigate their synergistic effects on hydration processes and strength development under low-temperature curing conditions. In the study of alkali-activated steel slag, a $Na_2O$ concentration of 4% and a water glass modulus of 1.5 were selected based on prior literature and preliminary experimental validation in our laboratory. According to previous studies, a $Na_2O$ concentration of 4% provides moderate alkalinity, effectively activating the steel slag without causing microstructural damage to the cement matrix. This concentration has been reported in the preparation of alkali-activated slag cement pastes (Sun et al., 2020; You et al., 2019).

## 2.2 Test methods

### 2.2.1 Setting time test

Setting time tests were conducted to investigate the setting behavior of cement pastes and evaluate the workability of the mixed paste. The setting time of the blended cement paste was determined using a Vicat apparatus, following the Chinese standard GB/T 1346-2011 (Standardization Administration of China, 2011). This standardized method ensures consistency and comparability of results, particularly when assessing the influence of steel slag powder on the setting behavior of cement paste. The blended cement paste was prepared by incorporating varying percentages of steel slag powder, as detailed in Table 2. The setting times were measured under controlled laboratory conditions, providing critical insights into the workability and early hydration characteristics of the cementitious system.

### 2.2.2 Activity index test

The activity index test was used to assess the contribution of steel slag powder to the mechanical strength of cement paste. The activity index of the steel slag powder was evaluated in accordance with the Chinese standard GB/T 12957-2005 (Standardization Administration of China, 2005). Mortar specimens were prepared by replacing 30% of the cement content with steel slag powder. The mortar mixes were produced using a water-to-binder ratio of 0.50 and placed in standard test cubic molds. The specimens were cured in a chamber maintained at 20°C ± 2°C and a relative humidity exceeding 95% to provide optimal conditions for hydration. After curing periods of 7 and 28 days, the compressive strengths of the specimens were tested and compared with reference specimens.

### 2.2.3 Hydration heat test

The hydration heat release behavior of steel slag cement pastes under low-temperature curing conditions was evaluated to understand the relationship between the hydration heat release curve and the hydration products. The hydration heat of the blended cement paste was measured using an isothermal conduction

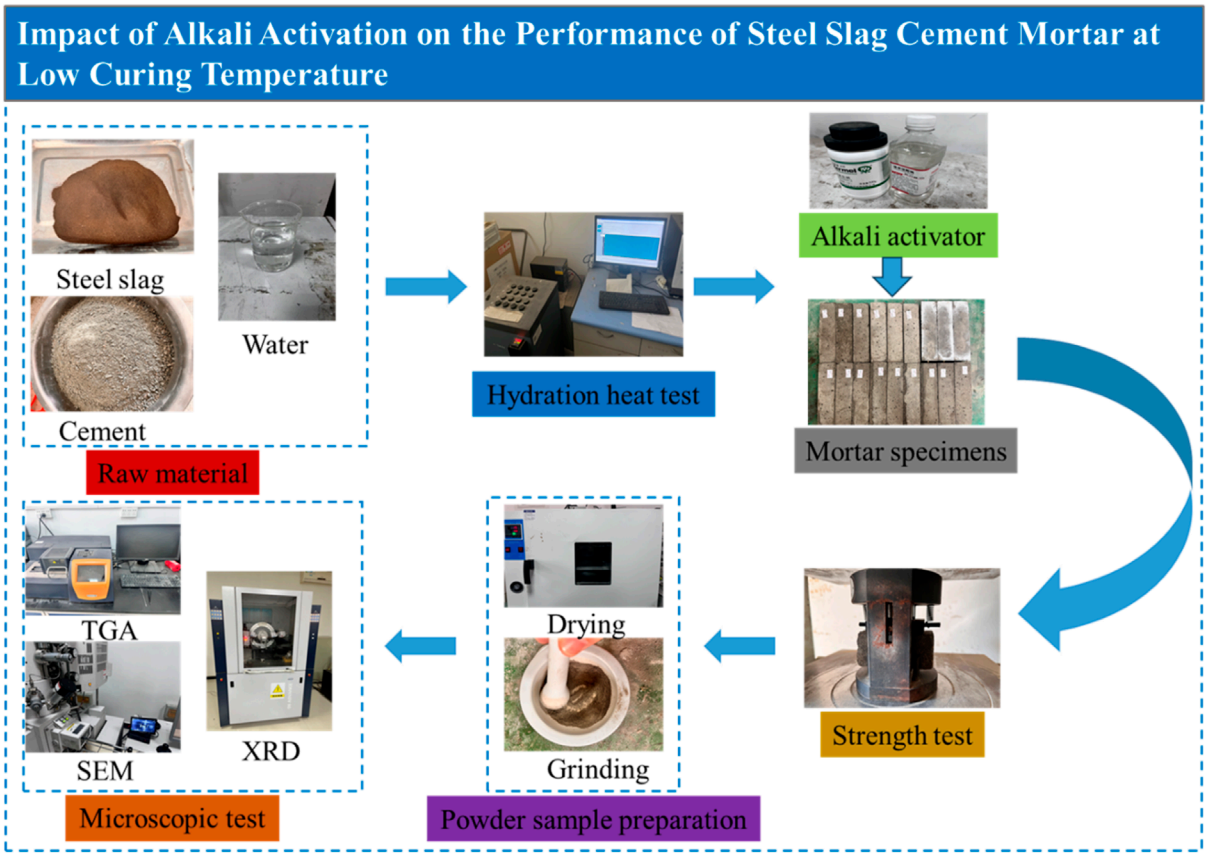


FIGURE 1
Experimental procedure for investigating the impact of alkali activation on the performance of steel slag cement mortar at low curing temperature.

TABLE 1 The main oxide of ordinary Portland cement and steel slag powder.

| Raw materials | Oxide (%) | | | | | | | | | |
|---|---|---|---|---|---|---|---|---|---|---|
| | CaO | $SiO_2$ | $Al_2O_3$ | $Fe_2O_3$ | MgO | $SO_3$ | $K_2O$ | $Na_2O$ | MnO | $P_2O_5$ |
| Ordinary Portland cement | 61.14 | 21.03 | 4.86 | 3.79 | 3.35 | 2.76 | 1.07 | 0.21 | 0.07 | 0.12 |
| Steel slag powder | 43.83 | 23.75 | 4.04 | 17.33 | 3.66 | 0.59 | 0.19 | 0.21 | 4.31 | 0.42 |

calorimeter at 10°C, for 168 h. The water-to-cement ratio of the paste was set at 0.45. Steel slag powder and cement were thoroughly mixed, followed by the addition of distilled water and stirring for 30 s to ensure uniformity. The prepared paste was then sealed in vials to prevent moisture loss and placed in the calorimeter for stabilization. Heat flow and cumulative heat release were continuously recorded, providing insights into the hydration kinetics and thermal characteristics of the blended cement system at low temperatures.

### 2.2.4 Mechanical strength test

Mechanical strength of the cement mortars was evaluated using compressive strength tests in order to evaluate the evolution of the properties with the hydration time for all the cement systems studied. Mortar mixes were prepared as specified in Tables 3 and 4. The dry components were mixed thoroughly, after which water and standard sand were added. The mortar was stirred at a slow speed for 2 min, followed by high-speed mixing for an additional 2 min to ensure a homogeneous mix. The prepared mortar was cast into molds and compacted to remove air voids. The molds were then placed in a curing chamber maintained at a temperature of 10°C ± 2°C and a relative humidity exceeding 95%. Compressive strength tests were conducted after curing for 3, 7, and 28 days, using a hydraulic testing machine manufactured in Wuxi, China, to evaluate the influence of steel slag and alkaline activators on the mechanical performance of the mortar. After the specific curing ages, solid samples of around 3 g were immersed in 50 mL of isopropanol to stop the hydration process and dried for 24 h.

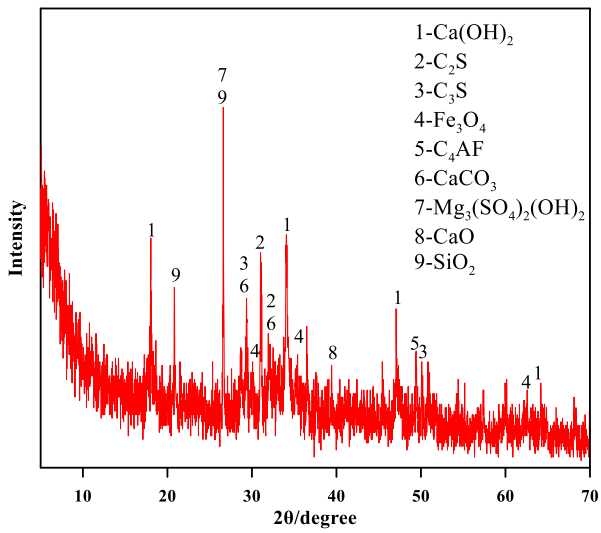


FIGURE 2
X-ray diffraction (XRD) pattern of steel slag powder.

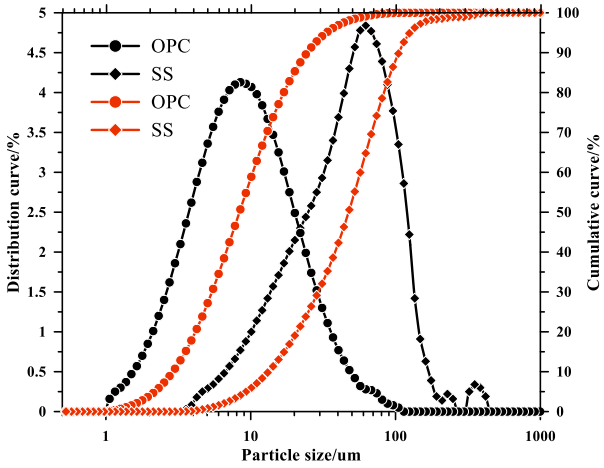


FIGURE 3
Particle size distribution of Portland cement and steel slag powder.

### 2.2.5 Thermogravimetric analysis (TGA)

Thermogravimetric analyses (TGA) were performed to analyze the thermal stability and decomposition of hydration products in the blended cement system, to quantify their mass loss with the increase in the temperature. For this characterization technique, samples were grounded into a fine powder, with a particle size of ≤75 μm). The TGA tests were conducted using a TA-Q5000 instrument under a high-purity nitrogen atmosphere. The samples were heated from 20°C to 1,000°C at a rate of 10°C per minute. The weight loss data were analyzed to identify phase transitions, such as the decomposition of calcium hydroxide and carbonates, providing insights into the hydration mechanisms.

### 2.2.6 X-ray diffraction (XRD)

X-ray diffraction (XRD) was utilized to identify the crystalline phases present in the hydrated cement paste, and to compare the results with those samples without alkaline activation and unhydrated. Dried and ground samples were analyzed using a Rigaku Max-2500VB X-ray diffractometer. Scans were conducted at a speed of 10°/min over a 2θ range of 5°–70°. The diffraction patterns obtained were used to monitor the formation of hydration products, and the remaining crystalline phases.

### 2.2.7 Scanning electron microscopy (SEM)

The microstructural morphology of hydration products of selected samples was observed using scanning electron microscopy (SEM), with a ZEISS Sigma 300 microscope. Fragments of solid samples were mounted on SEM stubs and polished with diamond pastes of ¼ micron. To enhance conductivity, the samples were coated with a thin layer of gold. The SEM analysis provided detailed observations of the microstructure, including the morphology of C-S-H and C-(N-)-A-S-H gels, calcium hydroxide crystals, and the overall compactness of the hydrated matrix.

## 3 Results and discussion

### 3.1 Characterization of setting behavior in blended cement paste

Figure 4 shows a comparison of the setting times of cement pastes incorporating different amounts of steel slag powder, and cured under low (10°C) and room-temperatures (20°C). The results suggested that the setting time progressively increases as the replacement level of steel slag rises. This behavior highlights how steel slag influences the hydration process of cementitious systems, driven by factors such as its chemical composition, mineralogical phases, fineness, alkalinity, water content and its interaction with other cement phases. (Mai et al., 2020).

One of this factor influencing the process is the increased water-to-cement ratio introduced by steel slag powder. The additional water creates a delay in the separation of cement particles from the water, thereby prolonging the initial and final setting times. Furthermore, the reduced proportion of reactive phases—particularly tricalcium silicate ($C_3S$) and dicalcium silicate ($C_2S$)—in steel slag leads to a significant decrease in hydration activity. Steel slag is rich in inert components such as MgO and $MnO_2$, which, while providing structural benefits, reduce the overall reactivity of the composite cementitious matrix (Bilim and Atiş, 2012; Monshi and Asgarani, 1999). This decrease in hydration reactivity results in a slower rate of heat evolution, which is critical for setting and hardening processes (Yi et al., 2012; Li et al., 2011).

The data indicate that under low-temperature curing conditions (10°C), the delays in setting times were more pronounced. For instance, initial setting times for cement pastes with steel slag replacement levels of 10%, 20%, and 30% increased by 11.0%, 24.2%, and 44.1%, respectively, compared to pure cement paste. Similarly, final setting times showed extensions of 17.9%, 22.7%, and 35.1% at the same replacement levels. These observations align with prior research, which attributes this delay to the dilution effect caused by reduced clinker content. Lower clinker content decreases the

TABLE 2 The mix proportion of sample.

| Sample | Steel slag powder/% | Cement/% | Curing temperature/°C |
|---|---|---|---|
| SS0 | 0 | 100 | 10 |
| SS10 | 10 | 90 | 10 |
| SS20 | 20 | 80 | 10 |
| SS30 | 30 | 70 | 10 |
| SS0 | 0 | 100 | 20 |
| SS10 | 10 | 90 | 20 |
| SS20 | 20 | 80 | 20 |
| SS30 | 30 | 70 | 20 |

TABLE 3 The amount of each material of single activator.

| Sample | $Na_2O$/% | Steel slag powder/g | Cement/g | Sand/g | Water/g | NaOH/g |
|---|---|---|---|---|---|---|
| 1 | 0% | 135 | 315 | 1,350 | 225 | 0 |
| 2 | 2% | 135 | 315 | 1,350 | 225 | 3.48 |
| 3 | 3% | 135 | 315 | 1,350 | 225 | 5.23 |
| 4 | 4% | 135 | 315 | 1,350 | 225 | 6.97 |
| 5 | 5% | 135 | 315 | 1,350 | 225 | 8.71 |
| 6 | 6% | 135 | 315 | 1,350 | 225 | 10.45 |

TABLE 4 The amount of each material of composite activator.

| Sample | $Na_2O$/% | Modulus | $Na_2SiO_3$/g | NaOH/g | Water/g | Steel slag powder/g | Cement/g | Sand/g |
|---|---|---|---|---|---|---|---|---|
| S2-M0.5 | 2% | 0.5 | 4.86 | 2.95 | 221.87 | 135 | 315 | 1,350 |
| S2-M1 | 2% | 1 | 9.71 | 2.42 | 218.74 | 135 | 315 | 1,350 |
| S2-M1.5 | 2% | 1.5 | 14.57 | 1.88 | 215.6 | 135 | 315 | 1,350 |
| S2-M2 | 2% | 2 | 19.42 | 1.35 | 212.48 | 135 | 315 | 1,350 |
| S4-M0.5 | 4% | 0.5 | 9.72 | 5.9 | 218.74 | 135 | 315 | 1,350 |
| S4-M1 | 4% | 1 | 19.42 | 4.83 | 212.48 | 135 | 315 | 1,350 |
| S4-M1.5 | 4% | 1.5 | 29.13 | 3.76 | 206.21 | 135 | 315 | 1,350 |
| S4-M2 | 4% | 2 | 38.83 | 2.69 | 199.96 | 135 | 315 | 1,350 |
| S6-M0.5 | 6% | 0.5 | 14.58 | 8.85 | 215.6 | 135 | 315 | 1,350 |
| S6-M1 | 6% | 1 | 29.13 | 7.25 | 206.21 | 135 | 315 | 1,350 |
| S6-M1.5 | 6% | 1.5 | 43.70 | 5.64 | 196.82 | 135 | 315 | 1,350 |
| S6-M2 | 6% | 2 | 58.25 | 4.04 | 187.43 | 135 | 315 | 1,350 |

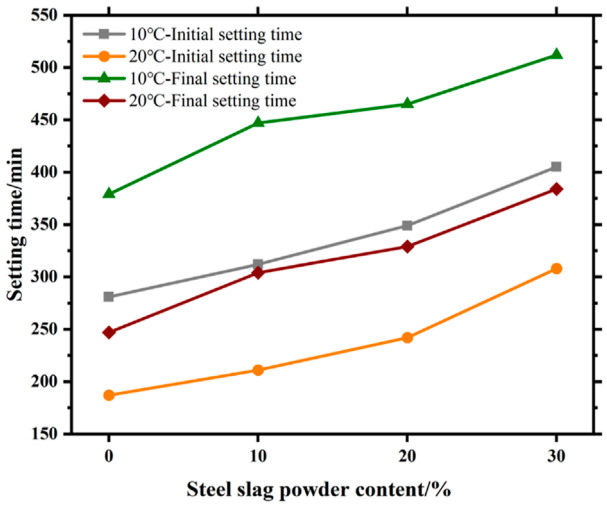


FIGURE 4
Setting time of mixed cement paste.

availability of reactive phases such as $C_3S$ and $C_2S$, which are essential for early hydration and strength development (Guo et al., 2018b; Xiong et al., 2022; Kua, 2015).

When comparing the effects of curing temperatures, the results demonstrate a clear exacerbation of delays at low temperatures. At 10°C, initial setting times increased by 47.9%, 44.2%, and 31.5% for steel slag replacement levels of 10%, 20%, and 30%, respectively, compared to room-temperature curing at 20°C. Final setting times also rose substantially under low-temperature curing, increasing by 47.0%, 41.3%, and 33.3%. These observations are consistent with prior studies reporting that lower temperatures significantly reduce molecular mobility and slow hydration reaction rates. At 10°C, the dissolution of reactive phases is inhibited, delaying the precipitation of critical hydration products such as calcium-silicate-hydrate (C-S-H) gels and calcium hydroxide ($Ca(OH)_2$) (Liu et al., 2020; Qasrawi et al., 2009). This slowdown in hydration activity extends both the setting and hardening processes, particularly in cold environments.

Another critical aspect of the retardation observed with steel slag is the role of its inert components, such as MgO, $MnO_2$, and the RO phase. These inert phases not only dilute the reactive content of the binder but also act as nucleation sites. This phenomenon alters the crystallization pathways of hydration products and further reduces the hydration rate (Monshi and Asgarani, 1999; Kua, 2015). The substitution of clinker with steel slag additionally decreases the heat released during hydration. This reduction in heat evolution is particularly detrimental under low-temperature conditions, where sufficient heat is crucial for accelerating hydration reactions and ensuring timely strength development (Li et al., 2011; Qasrawi et al., 2009).

The interaction between steel slag content and curing temperature emerges as a key factor influencing the setting behavior and hydration kinetics of blended cement pastes. While the use of steel slag provides significant environmental benefits, such as reducing clinker consumption, lowering $CO_2$ emissions, and promoting the recycling of industrial by-products, its incorporation requires thoughtful adjustments to mix design and curing protocols. For instance, optimizing the particle size distribution of steel slag could enhance its reactivity by increasing the surface area available for hydration. The addition of chemical activators, such as alkali or sulfate-based compounds, could further improve the early-age performance of steel slag-blended systems. Combining steel slag with other reactive supplementary cementitious materials (SCMs) like fly ash or metakaolin might also offset the retardation effects while maintaining sustainability goals (Xue et al., 2006).

Moreover, tailoring curing protocols becomes particularly critical in low-temperature environments. Strategies such as insulating formwork, applying external heating, or preheating the mixing water could mitigate the adverse effects of low curing temperatures on the hydration process (Fang et al., 2018). These measures, combined with careful mix design, can enhance the setting characteristics and overall performance of steel slag-based cementitious systems in cold climates.

From a sustainability perspective, the utilization of steel slag aligns with global efforts to reduce the carbon footprint of the construction industry. However, as the findings of this study illustrate, achieving a balance between environmental benefits and practical performance requirements is essential (Provis et al., 2015). The prolonged setting times observed with higher levels of steel slag replacement, particularly under low-temperature conditions, emphasize the importance of addressing performance trade-offs through innovative solutions.

## 3.2 Assessment of the activity index for steel slag powder

In accordance with relevant standard, the activity index is generally expressed as the compressive strength ratio $K$. The calculation method for the coefficient $K$ is outlined in Equation 1.

$$K = \frac{C_1}{C_2} \times 100 \quad (1)$$

where, $K$ is the compressive strength ratio, unit is percentage (%); $C_1$ is the compressive strength of the sample containing steel slag powder; $C_2$ is the compressive strength of the control group sample.

The compressive strength, flexural strength, and activity index of the steel slag cement mortar are presented in Figure 5. The activity indexes for the steel slag powder were measured to be 46.01%, 64.71%, and 72.21% at 3, 7, and 28 days, respectively. These results demonstrate the relatively high pozzolanic activity of the steel slag powder, which contributed to a notable increase in the strength of the steel slag cement mortar (Cai et al., 2024).

The progression of the activity index over time indicates the gradual and sustained reactivity of the steel slag powder. At 3 days, the activity index (46.01%) reflects the limited contribution of steel slag powder to early hydration, likely due to the slower dissolution of reactive phases such as tricalcium silicate ($C_3S$) and dicalcium silicate ($C_2S$) in the slag. However, at 7 and 28 days, the activity indexes increase to 64.71% and 72.21%, respectively, indicating that the hydration of steel slag powder becomes more effective over time. This delayed but sustained reactivity is advantageous for applications requiring controlled heat evolution during hydration, such as in mass concrete structures, where

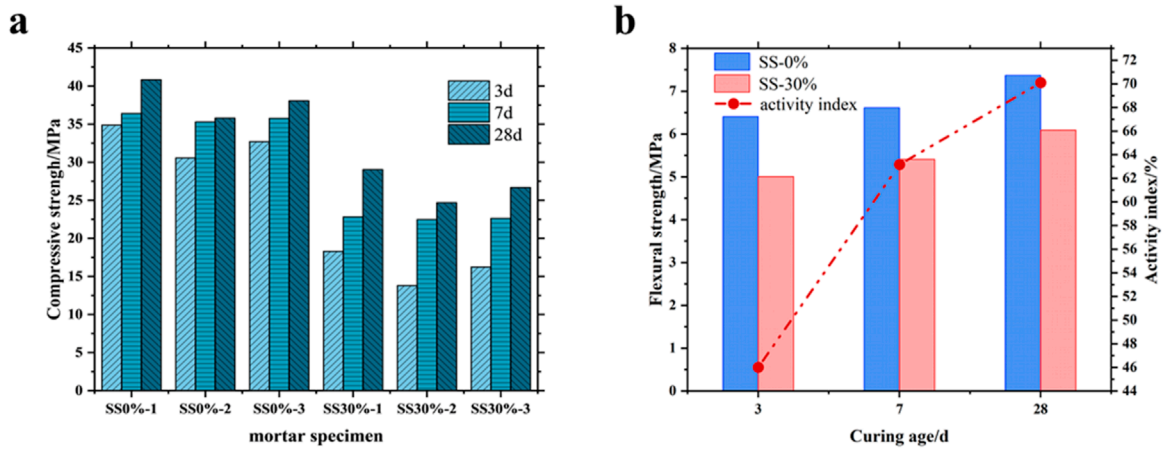


FIGURE 5
**(A)** Compressive strength of cement mortar with 0% and 30% steel slag powder **(B)** Flexural strength and activity index of cement mortar with 0% and 30% steel slag powder.

excessive heat buildup may lead to thermal cracking (Zhou et al., 2023). The enhanced reactivity of steel slag powder facilitates the formation of secondary hydration products, such as calcium-silicate-hydrate (C-S-H) gels, which contribute to the densification of the cementitious matrix, improving both strength and durability. The C-S-H formed in alkali-activated steel slag cement paste differs significantly from that in conventional cement hydration. In alkali-activated systems, the C-S-H structure is more highly cross-linked and compact, typically exhibiting a lower Ca/Si ratio with the incorporation of Na and Al ions, forming a C-(N)-A-S-H type gel (Marvila et al., 2021; Richardson, 2008). In contrast, C-S-H in conventional cement hydration tends to form a more open and porous morphology than the C-(N)-A-S-H gel, contributing to differences in mechanical properties and durability between plain and alkaline activated cements.

The relatively high activity of the steel slag powder used in this study brings several benefits to cementitious materials: as (a) improved strength by the formation of additional C-S-H gels and other hydration products significantly enhances both compressive and flexural strengths of the steel slag cement mortar; (b) sustained hydration with the ongoing reactivity of steel slag powder supports continued hydration, resulting in strength gains over an extended period, this property is crucial for ensuring long-term structural performance (Wei et al., 2024); (c) reduced clinker content by replacing clinker with steel slag powder, the overall cement content can be reduced without compromising performance, contributing to lower $CO_2$ emissions and improved resource efficiency in cement production; and (d) enhanced durability since the activity of steel slag powder improves the microstructure by reducing porosity and refining pore size distribution, thus enhancing resistance to shrinkage, cracking, and chemical attack (Sheng et al., 2023).

Optimizing the activity of steel slag powder is essential for achieving superior performance in blended cement systems. Several approaches can be employed to enhance its activity, including: particle size reduction, grinding steel slag to a finer particle size increases the surface area (Sengupta et al., 2024), thereby accelerating its hydration rate and improving its reactivity; chemical activation, the use of chemical activators, such as alkali or sulfate-based compounds, can stimulate the reactivity of steel slag powder, particularly in early hydration stages; and thermal processing, heat treatment of steel slag can modify its mineralogical phases, improving the reactivity of otherwise inert components.

Additionally, optimizing curing conditions, particularly in colder environments, may further enhance the performance of steel slag cement mortars. For instance, preheating mixing water or insulating formwork can mitigate the slower hydration rates associated with low temperatures, ensuring consistent strength development.

## 3.3 Evaluation of hydration heat behavior

Under low-temperature conditions, the incorporation of steel slag powder significantly influences the hydration heat release process of cement pastes. Figure 6 demonstrates that at a constant curing temperature of 10°C, the hydration heat release rate follows a characteristic trend: a sharp initial rise, followed by a gradual decline, while the cumulative hydration heat consistently increases over time (Joseph and Cizer, 2022). However, as steel slag powder content increases, both the peak hydration heat release rate and the time to reach this peak are adversely affected. Specifically, at slag powder contents of 0%, 10%, 20%, and 30%, the maximum heat release rates were measured at 0.93, 0.82, 0.72, and 0.63 mW, respectively. Furthermore, the time to reach these peaks was progressively delayed to 19.73, 20.55, 20.86, and 21.43 h, indicating a slower overall hydration process. The cumulative heat release over 7 days also exhibited a declining trend, with values of 175.18, 155.87, 138.71, and 126.38 J/g, respectively. These results underscore that the inclusion of steel slag powder, particularly at higher dosages, not only reduces the rate of hydration heat release but also significantly slows the hydration kinetics (Sheng et al., 2023). The activation energy ($E_a$) of alkali-activated steel slag systems is typically higher than that of conventional Portland cement due to the complex dissolution and polycondensation processes involved.

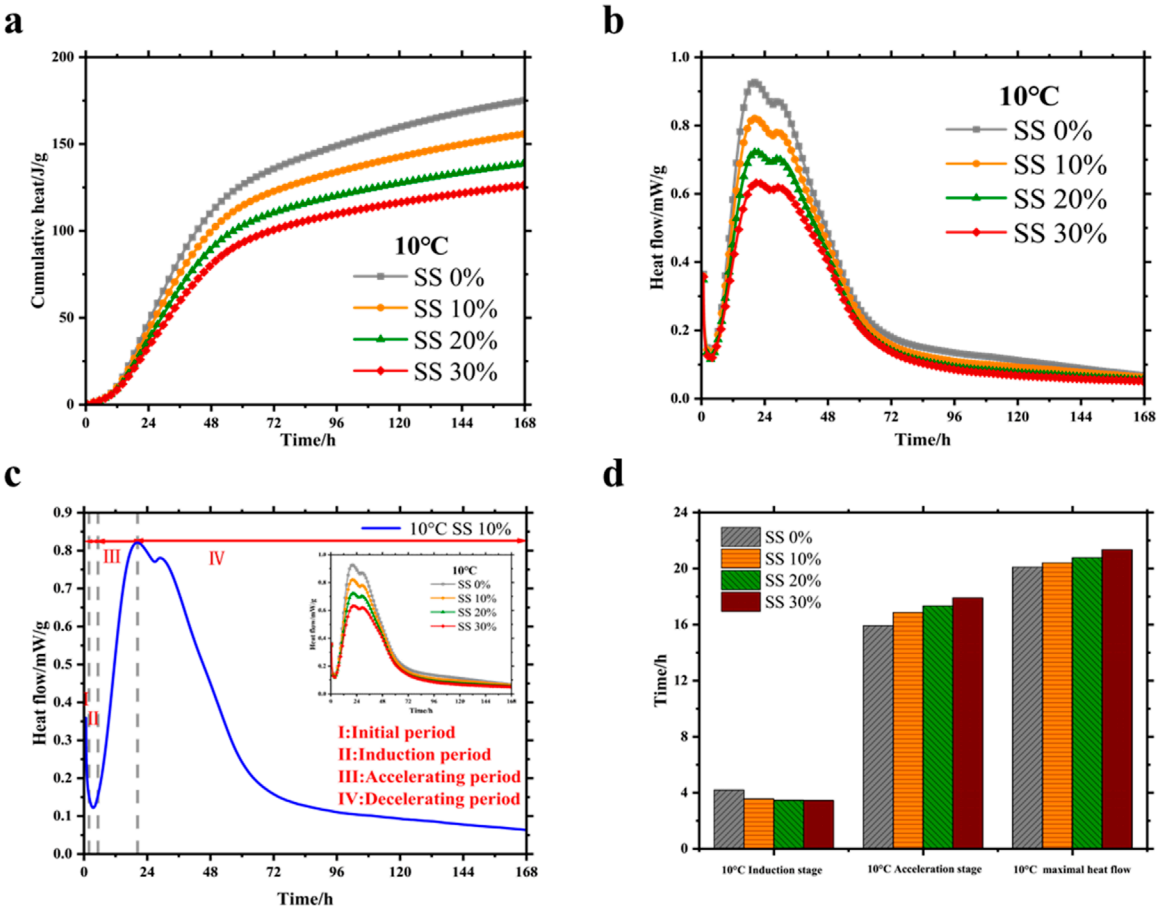


FIGURE 6
Results of hydration heat experiment. **(A)** Hydration flow. **(B)** Cumulative heat, Characteristics of hydration heat behavior. **(C)** Schematic diagram of cement hydration stage at early age. **(D)** Critical time points in the hydration process.

Previous studies report activation energy values ranging from 60 to 80 kJ/mol for alkali-activated slag, compared to 40–50 kJ/mol for Portland cement (Provis, 2014; Shi et al., 2003). This higher activation energy explains the reduction in reaction rates at lower temperatures, such as 10°C, as more thermal energy is required to overcome the reaction barrier.

The reduction in hydration heat release and delayed peak times can be attributed to several mechanisms (Li et al., 2023). First, steel slag powder possesses relatively low hydration reactivity due to its mineralogical composition, which typically includes inert or less reactive phases such as magnesium oxide (MgO), manganese oxide ($MnO_2$), and RO phases. These components dilute the reactive tricalcium silicate ($C_3S$) and dicalcium silicate ($C_2S$) phases in cement, which are primarily responsible for the heat evolution during hydration (Zhou et al., 2023). The dilution effect reduces the overall availability of reactive phases, leading to a lower hydration rate and diminished heat generation. The initial period corresponds to the rapid dissolution of steel slag particles, releasing $Ca^{2+}$ and $Al^{3+}$ ions into the solution, which is crucial for initiating the hydration reaction. During the induction period, the solution becomes supersaturated with respect to the reaction products. This stage is characterized by the nucleation of C-S-H gel, as evidenced by the formation of early amorphous phases in the XRD patterns. The main reaction peak corresponds to the primary stage of the hydration process, where a substantial amount of C-S-H gel precipitates and interconnects with the possible incorporation of Na and Al ions to form C-(N)-A-S-H gel. The formation of a dense and continuous microstructure, as observed in SEM images, further supports this phenomenon with the formation of gels densifying the hydration products matrix. Moreover, part of the inert nature of steel slag particles can inhibit the nucleation and growth of hydration products, further delaying the hydration process (Zhang et al., 2023).

The exothermic hydration reaction in cement typically proceeds through four distinct stages: initial dissolution, induction, acceleration, and deceleration. While the inclusion of steel slag powder does not fundamentally alter these stages, it significantly affects their duration and the corresponding reaction rates. In particular, during the induction period, higher slag content reduces the reaction rate, as the less reactive slag particles delay the release of ions and the formation of initial hydration products (Ren et al., 2024). As a result, the induction period becomes shorter with increasing slag content. Low curing temperatures exacerbate this effect by further reducing molecular mobility and slowing ion diffusion, thereby extending the overall hydration process. At 10°C,

both the dissolution of slag and the formation of C-S-H gels occur at a significantly slower rate. This reduction in reaction kinetics can be described using Arrhenius-type relationships, wherein the reaction rate constant ($k$) decreases exponentially as temperature decreases (Bernal et al., 2011; Shi and Fernández-Jiménez, 2006).

During the acceleration phase, the effects of both low temperature and increased slag content become more pronounced. Low temperatures reduce the rate of hydration product formation, such as calcium-silicate-hydrate (C-S-H) gels, which are critical for matrix densification and strength development (Fang et al., 2023). Furthermore, as slag content increases, the duration of the acceleration phase is extended. This can be attributed to the reduced heat generation and slower reaction kinetics (Li et al., 2023), which create favorable conditions for sustained hydration over an extended period. While this prolonged acceleration phase may be beneficial for long-term strength development, it also delays the peak heat release time and prolongs the setting and early hardening stages, which may be a limitation in time-sensitive construction projects.

The delayed heat release peak time is a critical indicator of the combined effects of curing temperature and slag powder content. As the curing temperature decreases, the peak time shifts further, reflecting the slower hydration reactions at low temperatures. This phenomenon highlights the interplay between the dilution effect of slag and the reduced reactivity of cementitious materials under cold conditions (Gholizadeh-Vayghan et al., 2024). The delayed reaction kinetics at 10°C result in a less dense and more porous microstructure during early hydration stages, as slower reaction rates limit gel formation and matrix densification (Provis and Bernal, 2014; Shi et al., 2011). However, alkali activation can partially mitigate the negative impact of low-temperature curing on strength development by enhancing the long-term reactivity of the system (Bernal et al., 2012). By analyzing key hydration time points—the end of the induction period, the duration of the acceleration phase, and the time to reach the peak heat release rate—it is possible to gain a comprehensive understanding of how slag content and curing conditions influence hydration kinetics and heat flow trends.

In addition to these time-dependent effects, the cumulative hydration heat provides valuable insights into the long-term impact of steel slag powder on the hydration process. The declining cumulative heat output with increasing slag content indicates that steel slag not only slows the rate of hydration but also limits the total heat generation over time. This behavior is particularly significant for applications in cold climates, where sufficient heat generation is crucial for maintaining adequate reaction rates and preventing delayed setting or early-age strength loss. In such scenarios, strategies to enhance the reactivity of slag powder, such as grinding to finer particle sizes, chemical activation, or blending with other reactive supplementary cementitious materials (SCMs), could mitigate the negative effects of high slag content and low temperatures.

Despite the slower hydration rates and lower heat generation associated with steel slag powder, its use in cementitious systems offers several potential benefits. For instance, the reduced peak heat release rate can be advantageous in mass concrete applications by minimizing thermal gradients and reducing the risk of thermal cracking (Usherov-Marshak et al., 2021). Furthermore, the slower hydration process associated with steel slag can lead to improved long-term strength and durability by facilitating a more gradual and uniform development of hydration products (Moon et al., 2018; Fang et al., 2024). The incorporation of steel slag also contributes to sustainability by reducing the reliance on clinker, lowering $CO_2$ emissions, and promoting the use of industrial by-products in construction materials. These findings highlight the complex relationship between slag content, curing temperature, and hydration kinetics. While higher slag content and low temperatures can impede the hydration process, careful adjustments to mixture design and curing protocols can optimize performance and ensure consistent material properties.

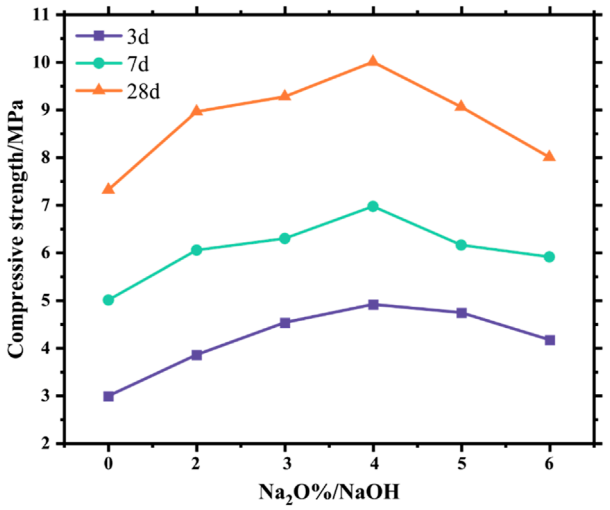


FIGURE 7
Compressive strength of steel slag cement mortar with different NaOH content.

## 3.4 Effect of NaOH on mechanical strength

To evaluate the effect of NaOH on the mechanical strength of composite cement mortar, the steel slag cement mortar formulation presented in Table 2 was utilized. The results of the mechanical strength tests for varying NaOH contents are illustrated in Figure 7. The control group, which lacks any activator, exhibits significantly lower mechanical strength compared to the groups with NaOH activation (Fang et al., 2024). This is primarily attributed to the inherently low hydration activity of steel slag powder, which contains minimal amounts of active components such as $C_2S$ and $C_3S$. In the absence of an effective activation mechanism, the steel slag powder remains largely unhydrated or undergoes only limited hydration over extended periods.

Under low-temperature curing conditions (10°C), the compressive strength of the steel slag cement mortar initially increases with higher NaOH content but subsequently declines, indicating the existence of an optimal dosage for NaOH as the sole activator. The results show that when the $Na_2O$ dosage is 4%, the compressive strength reaches its peak across all curing ages. Compared to the control group, the 3-day, 7-day, and 28-day compressive strengths for a 4% $Na_2O$ dosage increased by

64.5%, 39.2%, and 36.7%, respectively, underscoring the significant impact of NaOH on the early-age compressive strength. Notably, the 3-day compressive strength showed the greatest improvement, highlighting NaOH role in accelerating early hydration reactions. However, the overall compressive strength remains relatively low when NaOH is used as the sole activator. Specifically, the 3-day compressive strength does not exceed 5 MPa, and the maximum 28-day strength reaches only around 10 MPa (Ji et al., 2024).

The observed improvements in strength can be attributed to the chemical role of the NaOH activator, which increases the $OH^-$ concentration in the hydration environment. This elevated $OH^-$ concentration promotes the depolymerization of the glassy structure of steel slag, enhancing the release of reactive ions and accelerating the hydration process (Sun et al., 2020). However, the reaction of $OH^-$ ions with $Ca^{2+}$ in the system results in the formation of $Ca(OH)_2$ crystals, which can accumulate and act as a barrier to further hydration. This accumulation limits the long-term hydration activity of steel slag, thereby reducing the enhancement effect of NaOH over time. Consequently, while NaOH improves early-age hydration, its impact diminishes in the later stages of curing (Ji et al., 2023).

Low-temperature curing conditions exacerbate the limitations of NaOH activation. At lower temperatures, nucleation and growth kinetics are significantly hindered, reducing the effectiveness of hydration reactions (Sun et al., 2020). According to the Arrhenius law, the chemical reaction rate is highly sensitive to temperature changes, as lower temperatures reduce the kinetic energy of molecules and slow the hydration process (Zhang et al., 2023; Liu et al., 2019; Ghorbani et al., 2023). In such environments, the reduced molecular motion diminishes the probability of effective molecular collisions and bond formation, thereby lowering the reaction rate over a given time. Additionally, the reduced kinetic energy under low-temperature conditions limits the diffusion of activator molecules, further restricting their ability to facilitate hydration. NaOH acts as an effective activator for steel slag cement mortar by enhancing early-age compressive strength, its overall impact is constrained by the accumulation of $Ca(OH)_2$ and the inhibitory effects of low-temperature curing. This highlight the need for combining NaOH with other activators or supplementary measures to overcome these limitations and achieve higher long-term strength under challenging curing conditions.

## 3.5 Effect of composite activator on mechanical strength

The mechanical performance of steel slag cement mortar activated with NaOH and water glass is illustrated in Figure 8, highlighting the influence of varying $Na_2O$ contents (2%, 4%, and 6%) and water glass moduli on compressive strength. At a $Na_2O$ content of 6%, the high water glass content required for the alkali solution results in a highly viscous slurry, making it impossible to form the S6-M2 mortar group. This indicates that higher activator content can negatively impact workability due to increased viscosity (Zhang et al., 2020; Huang et al., 2019).

Under low-temperature curing conditions (10°C), compressive strength increases with a rise in the water glass modulus when $Na_2O$ content is fixed. Conversely, when the water glass modulus is constant, compressive strength increases with higher $Na_2O$ contents (Escalante-Garcia, 2003). For instance, at 4% $Na_2O$, the 28-day compressive strength of mortars with water glass moduli of 0.5, 1, 1.5, and 2 increased by 180%, 186.6%, 196.3%, and 202.1%, respectively, compared to the control group. Similarly, at a fixed water glass modulus of 1.5, the 28-day compressive strength of mortars with $Na_2O$ contents of 2%, 4%, and 6% increased by 75.8%, 196.3%, and 232.5%, respectively, over the control group. These trends demonstrate the synergistic effects of NaOH and water glass in enhancing hydration activity and improving strength development. The early strength gain is attributed to the formation of initial C-S-H gel and the partial polymerization of the aluminosilicate network. The continued increase in strength results from the progressive polycondensation of the aluminosilicate network and the formation of secondary phases, such as hydrotalcite-like phases, which fill residual pores and contribute to further matrix densification. This process is evidenced by the gradual reduction in porosity and the enhanced microstructural homogeneity observed in SEM images. The dense and uniform microstructure observed at 28 days aligns with the high compressive strength values presented in Figure 8.

The introduction of water glass enhances the hydration mechanism through multiple pathways. Water glass creates a highly alkaline environment, which accelerates the depolymerization of tetrahedral $[SiO_4]$ and $[AlO_4]$ structures in steel slag cement. This process releases reactive silica and alumina species that actively participate in hydration reactions (Zhang et al., 2017). Additionally, water glass supplies $Na_2SiO_3$, which reacts with $Ca(OH)_2$ to form calcium silicate hydrate (C-S-H) gels. $Na_2SiO_3$, characterized by its high polymerization degree, provides a robust structural framework for hydration products (Zhou et al., 2023). This framework enables hydration products such as C-S-H and calcium aluminate gels to embed within the matrix, filling voids and densifying the mortar, resulting in substantial compressive strength improvements.

At a $Na_2O$ content of 2%, the compressive strength remains relatively low, with 3-day strengths ranging between 4 and 6 MPa and 28-day strengths around 13 MPa. Increasing the $Na_2O$ content to 4% significantly enhances compressive strength, with 28-day values reaching 22.1 MPa. However, at 6% $Na_2O$, the compressive strength gain becomes less pronounced, achieving a 28-day strength of 24.3 MPa. This indicates diminishing returns in strength improvement at higher $Na_2O$ contents, likely due to a combination of factors, including reduced workability, oversaturation of silica, and localized accumulation of hydration products (Guan et al., 2021).

As $Na_2O$ content and water glass modulus increase, the ratio of cementitious material to activator decreases. The additional silica provided by water glass enhances the formation of hydration products, particularly C-S-H. However, at higher dosages, the excess silica does not proportionally contribute to strength development and may instead lead to inefficiencies in the hydration process (Liu et al., 2024). Excessive activator levels can also hinder hydration homogeneity, reducing the uniform distribution of hydration products and limiting further strength gains (Ma et al., 2018).

The dependency of compressive strength on both activator content and modulus highlights the importance of balancing these parameters. Higher $Na_2O$ content accelerates early hydration by increasing $OH^-$ concentration, promoting the dissolution of reactive

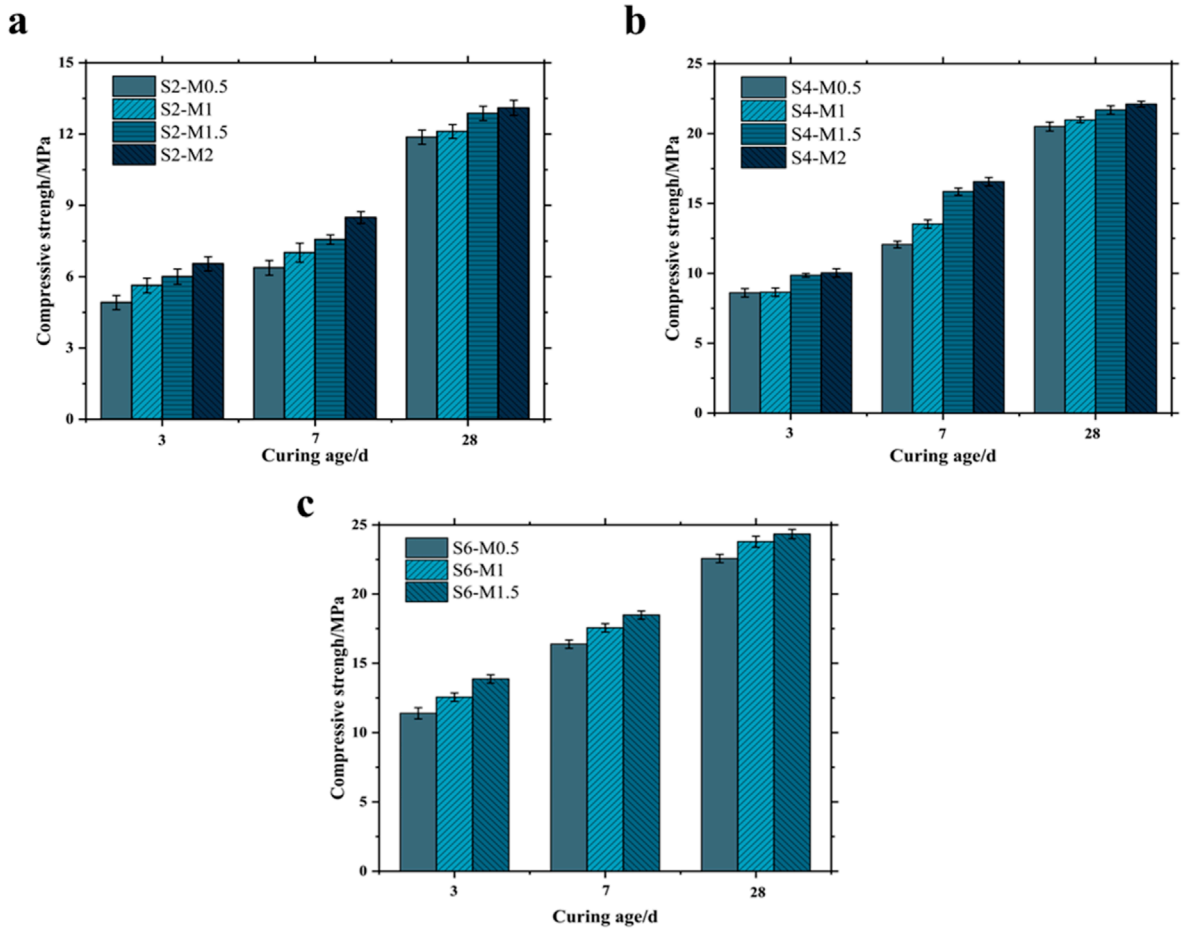


FIGURE 8
Compressive strength of steel slag cement mortar activated by a composite activator. **(A)** Sample with 2% $Na_2O$ content, **(B)** Sample with 4% $Na_2O$ content, **(C)** Sample with 6% $Na_2O$ content.

components in steel slag (Yang et al., 2023). However, the sustained supply of reactive silica from water glass moduli ensures continued hydration and densification of the matrix at later stages. This balance between early and sustained hydration activity is critical for optimizing the mechanical performance of steel slag cement mortar.

## 3.6 TG analysis

Figure 9A presents the TG and DTG curves of the slurry with and without the optimal activator under curing conditions of 10°C ± 2°C. As identified in previous studies, distinct thermal events are observed at specific temperature ranges: the peak near 100°C corresponds to the dehydration of calcium silicate hydrate (C-S-H) and ettringite (AFt); the peak at 400°C–500°C is associated with the dehydration of calcium hydroxide ($Ca(OH)_2$); and the peak at 630°C–750°C is due to the decomposition of calcium carbonate ($CaCO_3$), formed through the carbonation of $Ca(OH)_2$.

Figure 9B illustrates a typical TG curve along with its first and second derivative curves. The calculation method for $Ca(OH)_2$ content was carried out as follows (He et al., 2023; He and Lu, 2023; He et al., 2024): (a) In the second derivative curve, relatively flat segments near 400°C and 450 °C were selected, and the corresponding slopes ($k_1$ and $k_2$), temperatures ($T_1$ and $T_2$), and respective mass values ($M_1$ and $M_2$) on the mass loss curve were determined; (b) the peak temperature ($T_p$) within the range of 400°C–500 °C on the first derivative curve was determined, and (c) the $Ca(OH)_2$ content (CH, %) in the hydration products at 7 and 28 days, was calculated using Equation 2:

$$CH = \frac{74.1}{18.0}\{[M_1 + k_1(T_P - T_1)] - [M_2 + k_2(T_P - T_2)]\} \quad (2)$$

where, 74.1 and 18.0 are the molar mass of Ca $(OH)_2$ and $H_2O$ respectively.

From Figure 9B, it is evident that the $Ca(OH)_2$ content in the paste with the optimal activator is consistently higher than in the control group at both 7 and 28 days under low-temperature curing conditions (10°C). The content of $Ca(OH)_2$ in the activated paste increased by 35.46% at 7 days and 30.94% at 28 days compared to the reference sample. The higher $Ca(OH)_2$ content indicates more complete hydration of the mixed slurry, which correlates with greater mechanical strength. This can be attributed to the alkaline activator, which raises the pH of the slurry, facilitates ion exchange, and accelerates hydration, thereby forming a greater volume of stable hydration products.

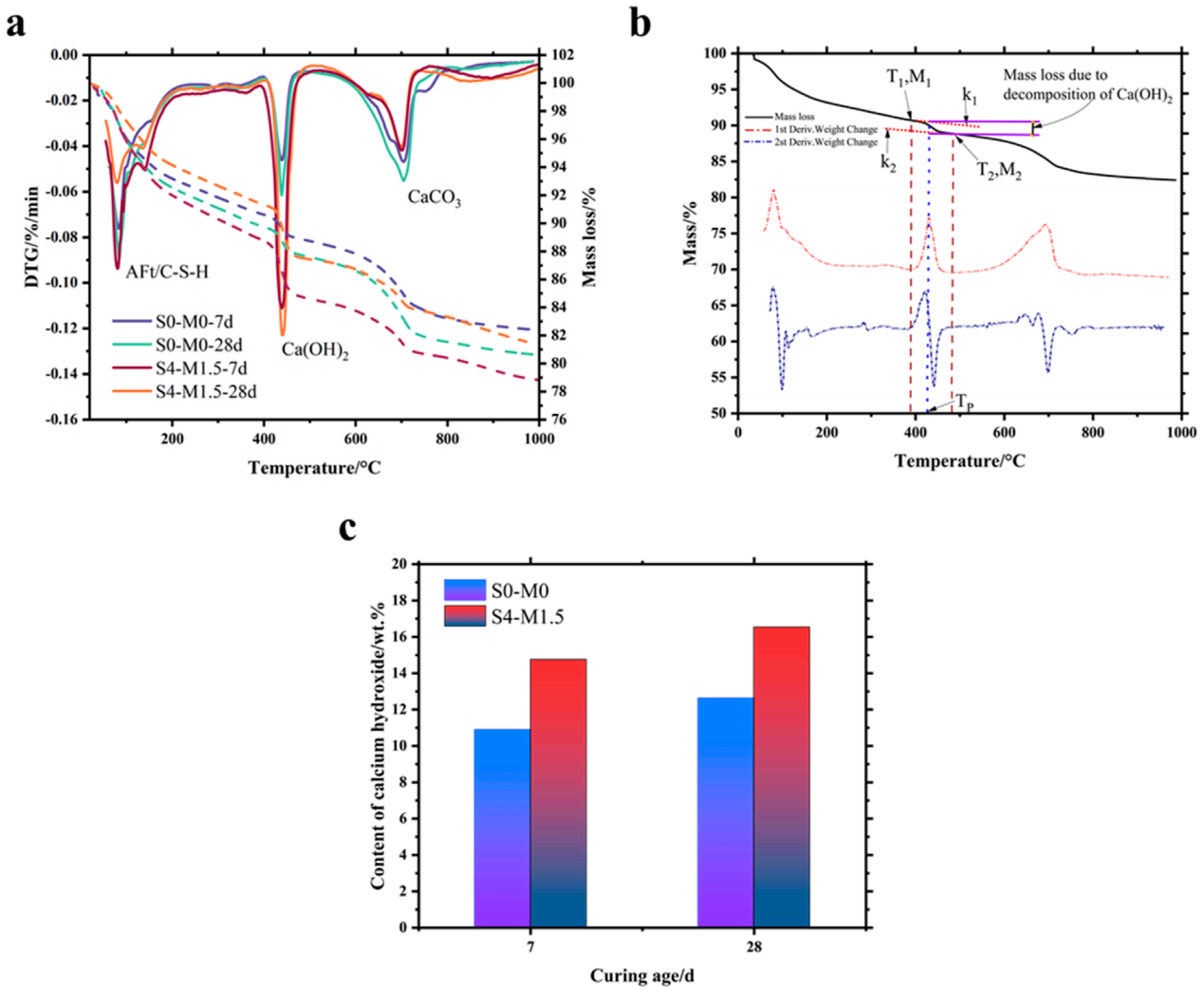


FIGURE 9
**(A)** The TG and DTG curves of different steel slag cement pastes. **(B)** Schematic diagram of the calculation method for $Ca(OH)_2$ content. **(C)** Comparison of $Ca(OH)_2$ content in different steel slag cement pastes.

The peaks observed in the TG and DTG curves demonstrate that while hydration reactions are inherently slower under low-temperature conditions, the addition of the alkaline activator mitigates this inhibitory effect. Low temperatures reduce molecular mobility, slowing the dissolution of reactive phases like tricalcium silicate ($C_3S$) and dicalcium silicate ($C_2S$) and limiting the formation of hydration products such as C-S-H and C-A-S-H gels (Bílek Jr et al., 2024). However, the alkaline environment introduced by the activator increases ion availability, enhances the dissolution of steel slag glassy phases, and promotes the growth of hydration products. As a result, despite the reduced intensity of hydration at low temperatures, the addition of the activator ensures more effective and complete hydration reactions.

The gradual increase in $Ca(OH)_2$ content over time further illustrates the sustained hydration activity facilitated by the activator. The formation of $Ca(OH)_2$, a by-product of cement hydration, is a key indicator of hydration progress and its effectiveness (Asaad et al., 2022; Gao et al., 2015). The elevated $Ca(OH)_2$ levels in the activated paste signify enhanced reactivity and improved thermal stability of the hydration products under low-temperature conditions. The activator not only accelerates the formation of C-S-H but also stabilizes the microstructure of the hydration products, reducing voids and increasing matrix density.

Under the combined influence of low-temperature curing and the alkaline activator, as shown in Figure 10, the hydration products of steel slag cement paste exhibit unique thermal behavior. While low temperatures inhibit hydration reactions, resulting in reduced weight loss during TG analysis, the activator compensates for this by promoting the formation of hydration products and improving their thermal stability (Gao et al., 2015). The presence of stable hydration products, such as C-S-H and C-A-S-H gels, leads to denser microstructures, which are critical for enhancing the mechanical performance of steel slag cement mortar.

The findings emphasize the role of the alkaline activator in overcoming the limitations imposed by low-temperature curing. By facilitating ion exchange and increasing the availability of reactive

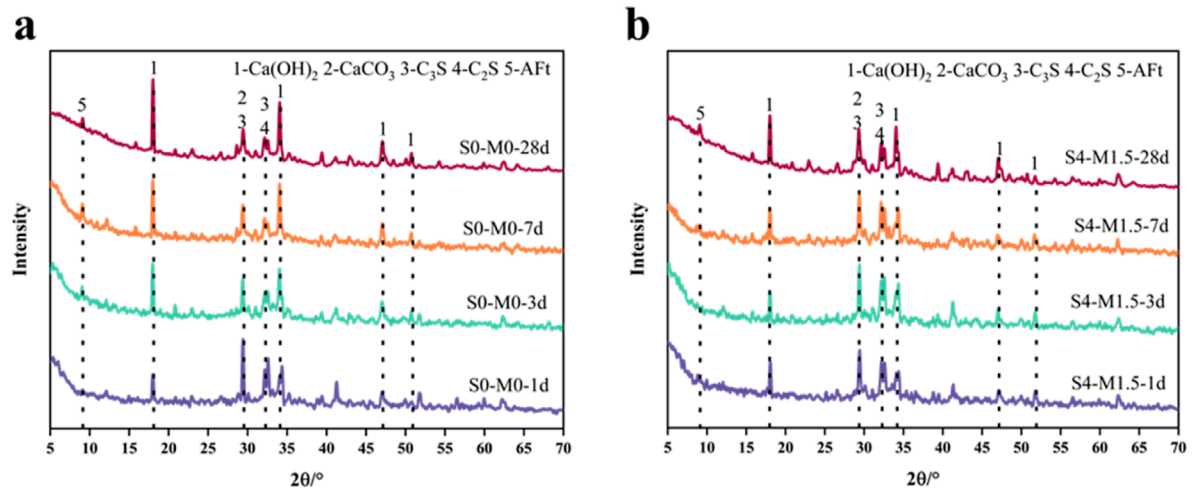


FIGURE 10
X-ray diffraction patterns of hydration products in steel slag cement paste. **(A)** Sample without alkaline activator, **(B)** Sample with optimally proportioned activator.

species, the activator significantly improves the completeness and thermal stability of the hydration process (Zhong et al., 2023). This improvement translates into enhanced strength and durability of the steel slag cement mortar, even under challenging curing conditions.

## 3.7 XRD analysis

Figure 10 presents the X-ray diffraction (XRD) patterns of hardened pastes containing 30% steel slag powder, cured at low temperatures (10°C) at different hydration ages, with and without the addition of an activator. The main diffraction peaks observed in both activated and non-activated samples are similar, including peaks for $Ca(OH)_2$, ettringite (AFt), and $CaCO_3$, as well as residual unhydrated clinker phases such as tricalcium silicate ($C_3S$) and dicalcium silicate ($C_2S$) (Ding et al., 2024). The presence of gypsum in the system facilitates the reaction of $C_3A$ with gypsum to form AFt (Sheng et al., 2023). As the curing age progresses, the diffraction peaks corresponding to hydration products become more pronounced, indicating the gradual development of hydration reactions over time (Jing et al., 2020).

In the non-activated samples, the $Ca(OH)_2$ diffraction peak shows notable variations with increasing curing age. These variations reflect the slower and less uniform hydration process in the absence of an activator. By contrast, the samples containing the optimal activator exhibit a higher degree of hydration as the curing age increases (Liu et al., 2024). This is accompanied by a more substantial reduction in the diffraction intensity of $C_3S$ and $C_2S$ peaks, indicating greater consumption of these primary clinker phases in the presence of the activator.

During the early stages of hydration, the $Ca(OH)_2$ diffraction peak is significantly stronger in the activated samples compared to the non-activated ones. This enhancement can be attributed to the alkaline activator, which accelerates the dissolution of $C_3S$ and $C_2S$, promoting the rapid formation of $Ca(OH)_2$. The activator increases the pH of the pore solution, enhancing the solubility of active components in the steel slag, such as $SiO_2$ and $Al_2O_3$ (Wang M. et al., 2024). These components react with $Ca(OH)_2$ to form secondary hydration products, including calcium silicate hydrate (C-S-H) and calcium aluminum silicate hydrate (C-A-S-H) gels.

In the later stages of hydration, the growth of the $Ca(OH)_2$ diffraction peak slows in the activated samples. This reduction in growth is due to the ongoing reaction between $Ca(OH)_2$ and the reactive phases of steel slag, leading to the formation of additional C-S-H and C-A-S-H gels. These secondary hydration reactions consume $Ca(OH)_2$, thereby lowering its concentration in the cement matrix over time (Stepkowska et al., 2007). This phenomenon demonstrates the efficiency of the alkaline activator in promoting the complete utilization of reactive components in steel slag powder, resulting in denser hydration products and improved microstructure (Wang M. et al., 2024).

The combined observations from the XRD patterns highlight the enhanced hydration kinetics and transformation of steel slag cement paste due to alkaline activation (Wang H. et al., 2024). The activator not only accelerates the dissolution of primary clinker phases and steel slag but also facilitates the formation of critical hydration products that contribute to improved mechanical strength and durability (Song et al., 2024). This enhanced reactivity underscores the importance of alkaline activators in optimizing the performance of steel slag cement systems under low-temperature curing conditions.

## 3.8 SEM analysis

Figure 11 shows scanning electron microscope (SEM) images of steel slag cement paste after 7 and 28 days of hydration, both with and without the addition of an activator. In the sample without the activator (Figures 11A,B), flocculent C-S-H gel and a small amount of plate-like $Ca(OH)_2$ are observed in the hydration products. At 7 days, the microstructure exhibits a limited quantity of C-S-H gel, with a large proportion of unhydrated steel slag particles and

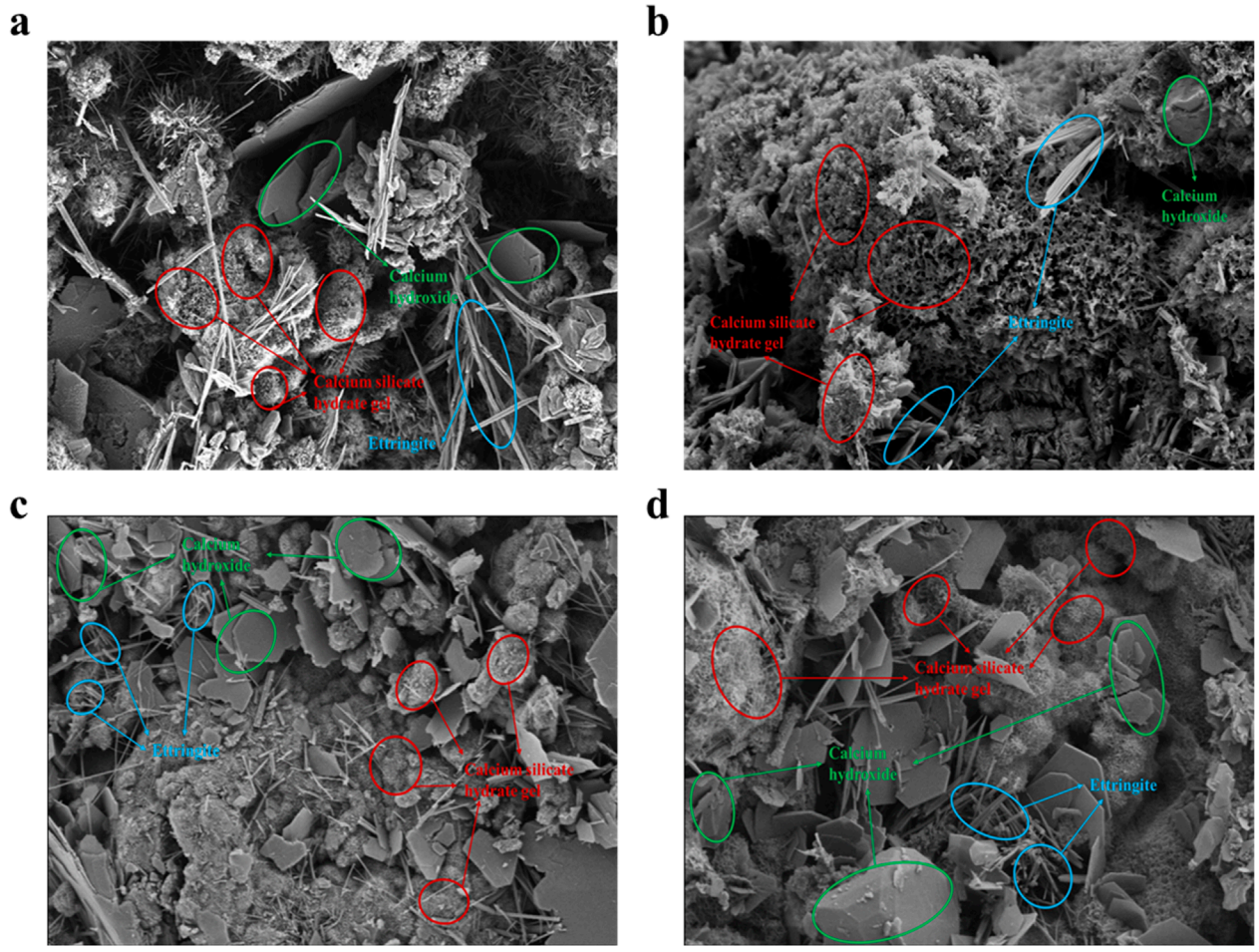


FIGURE 11
Scanning electron microscope images of steel slag cement paste after hydration. **(A)** 7 days without activator, **(B)** 28 days without activator, **(C)** 7 days with optimally proportioned activator, **(D)** 28 days with optimally proportioned activator. Scale bars: 5 μm; Magnification: 2.00 kX.

visible pores (Sun et al., 2020). The loose and porous structure results in lower mechanical strength at this early stage. By 28 days, the quantity of C-S-H gel increases, and the hydration products begin to intertwine and bond, leading to a denser structure compared to the 7-day sample. However, the overall number of hydration products remains relatively small, and the matrix is less compact compared to the activated sample.

In contrast, the sample with the activator (Figures 11C,D) shows a significantly enhanced microstructure. At 7 days, a larger quantity of flocculent C-S-H gels is observed, accompanied by a small amount of rod-like AFt crystals and flake-like hydration products (Zhang et al., 2023). The microstructure is notably more compact, with fewer visible pores and a denser matrix compared to the non-activated sample. By 28 days, the microstructure exhibits a high density of intertwined flocculent C-S-H gels, reduced quantities of plate-like $Ca(OH)_2$, and fewer rod-like AFt crystals. The number of flake-like hydration products decreases significantly as hydration progresses. Hydration products cross-link with unhydrated steel slag particles, cement particles, and AFt crystals, forming a solid and cohesive structure (Sun et al., 2020). The C-S-H-type (incorporating Al and Na ions) gel in alkali-activated steel slag cement paste mainly exhibits an amorphous or low-crystallinity dense structure. The incorporation of silicon, sodium and aluminum ions facilitates the formation of a uniform network with smaller particle sizes and a more homogeneous distribution, closely integrated with secondary phases such as hydrotalcite-like phases and (C-(N)-A-S-H)-type gels (Myers et al., 2013; García-Lodeiro et al., 2011).

The addition of the alkaline activator plays a pivotal role in improving the hydration process and microstructure of steel slag cement paste. The activator enhances the alkaline environment, which disrupts the reticular vitreous structure of steel slag and promotes the continuous formation of C-S-H gel. Water glass provides $OH^-$ and $SiO_3^{2-}$ ions to the system, accelerating the dissolution of the glassy phases in steel slag. $OH^-$ ions facilitate the disintegration of the steel slag vitreous structure, while $SiO_3^{2-}$ ions react with hydration products to form additional C-S-H gel. $Na^+$ ions further enhance the process by breaking down the network structure of the slag into highly active ionic groups, thereby improving the density and cohesiveness of the matrix microstructure (Liu et al., 2019; Ghorbani et al., 2023).

The chemical interactions among these ions enhance the hydration process, leading to the formation of a more compact matrix. The densification of the matrix in alkali-activated steel slag cement paste is further enhanced by the formation of secondary phases, including hydrotalcite-like phases and aluminosilicate gels (N-A-S-H), which occupy the interstitial spaces between C-S-H gel particles (Zhang et al., 2024; Zhang and Niu, 2023). These secondary phases contribute to a more compact and less permeable microstructure, thereby improving the mechanical properties and durability of alkali-activated cement-based materials, rendering them superior to conventional cementitious systems (Provis et al., 2015; Bernal et al., 2011). The optimization of the matrix microstructure is critical for improving the mechanical properties and durability of the paste (Zhang et al., 2017; Zhang et al., 2018). SEM images of the activated samples reveal a substantial increase in the length, quantity, and density of fibrous C-S-H gels compared to non-activated materials (Zhang et al., 2021). This demonstrates that the alkaline activation environment accelerates hydration reactions and promotes the formation of more stable gel phases. The reduction in the number of unhydrated particles further indicates a more complete hydration process in alkaline-activated systems, improving material utilization efficiency and contributing to the development of a denser, stronger steel slag cement paste structure.

## 4 Conclusion

In this study, the mechanical strength of steel slag cement mortar, along with the hydration products and microstructure of steel slag cement paste, was analyzed under low-temperature curing conditions using an alkaline activator. The main conclusions drawn are as follows:

1. The setting time of the slurry was reduced by both low-temperature curing and the increase in steel slag powder content. The addition of steel slag powder decreased the hydration rate of the composite system, resulting in slower heat release com-pared to pure cement paste. Low-temperature curing further slowed molecular movement, reducing hydration heat release and prolonging the setting time.
2. The optimal dosage of the NaOH activator was found to correspond to a 4% $Na_2O$ content. The use of a composite activator (NaOH + $Na_2SiO_3$) significantly enhanced the mechanical strength of steel slag cement mortar. Specifically, the mechanical strength increased with both higher $Na_2O$ content and an elevated water glass modulus, demonstrating the effectiveness of the composite activator in im-proving performance.
3. The optimum composition for the composite activator (NaOH + $Na_2SiO_3$) was determined to be 4% $Na_2O$ with a water glass modulus of 1.5. At this ratio, the activator efficiently enhanced the hydration reaction of steel slag cement paste, maintaining good fluidity and workability. This facilitated the development of a dense microstructure and improved mechanical properties. However, exceeding the optimal $Na_2O$ content or water glass modulus significantly increased the alkalinity of the system, accelerating hydration excessively. This rapid water consumption led to premature setting, negatively affecting the workability of the pastes.
4. Thermogravimetric analysis indicated that the mixed slurry with the optimal activator produced a greater volume of hydration products. The addition of the alkaline activator increased the pH of the paste, enhancing the dissolution of active components in steel slag powder and strengthening ion exchange. This process accelerated calcium ion release and facilitated the stable formation of hydration products. The activator also lowered the activation energy, accelerating hydration kinetics and promoting the rapid formation of early hydration products such as $Ca(OH)_2$. These hydration products improved paste density, contributing to enhanced mechanical properties and durability.
5. The hydration products of steel slag cement paste, both with and without the activator, were qualitatively similar. However, in the system containing the alkaline activator, the early hydration phase exhibited a marked increase in the intensity of the $Ca(OH)_2$ peak. This increase was attributed to the alkaline environment promoting the dissolution and release of calcium from the slag, resulting in higher $Ca(OH)_2$ formation. Additionally, the presence of the activator accelerated early hydration reactions, leading to a faster rate of $Ca(OH)_2$ formation.
6. Scanning electron microscopy analysis demonstrated that the activator disrupted the reticular vitreous structure of the steel slag, enabling more complete hydration. The microstructure of the activated slurry was notably more compact, characterized by a dense network of flocculent C-S-H gels and $Ca(OH)_2$. The incorporation of alkaline activators resulted in the formation of additional hydration products, effectively filling the pores, reducing porosity, and improving the overall material density.

## Data availability statement

The original contributions presented in the study are included in the article/supplementary material, further inquiries can be directed to the corresponding authors.

## Author contributions

WY: Methodology, Writing–original draft. TF: Investigation, Resources, Writing–original draft. WS: Formal Analysis, Methodology, Software, Writing–review and editing. LG: Formal Analysis, Methodology, Software, Writing–review and editing.

## Funding

The author(s) declare that financial support was received for the research and/or publication of this article. This research was funded by the Science and Technology R&D Program of Xinjiang Transportation Investment (Group) Co., Ltd (ZKXFWCG-202211-011): Research and Application of Comprehensive Utilization Technology for Steel Slag in Xinjiang Pavements.

## Conflict of interest

Author WY was employed by Xinjiang Jiaotou Construction Management Co., Ltd.

The remaining authors declare that the research was conducted in the absence of any commercial or financial relationships that could be construed as a potential conflict of interest.

The authors declare that this study received funding from Xinjiang Transportation Investment (Group) Co., Ltd. The funder had the following involvement in the study: providing steel slag raw materials for experiments and reviewing preliminary results for technical accuracy.

## Generative AI statement

The author(s) declare that no Generative AI was used in the creation of this manuscript.

## Publisher's note



## References

Asaad, M. A., Huseien, G. F., Memon, R. P., Ismail, M., Mohammadhosseini, H., and Alyousef, R. (2022). Enduring performance of alkali-activated mortars with metakaolin as granulated blast furnace slag replacement. *Case Stud. Constr. Mater.* 16, e00845. doi:10.1016/j.cscm.2021.e00845

Atiş, C. D., Bilim, C., Çelik, Ö., and Karahan, O. (2009). Influence of activator on the strength and drying shrinkage of alkali-activated slag mortar. *Constr. Build. Mater.* 23 (1), 548–555. doi:10.1016/j.conbuildmat.2007.10.011

Bernal, S. A., De Gutiérrez, R. M., and Provis, J. L. (2012). Engineering and durability properties of concretes based on alkali-activated granulated blast furnace slag/metakaolin blends. *Constr. Build. Mater.* 33, 99–108. doi:10.1016/j.conbuildmat.2012.01.017

Bernal, S. A., Provis, J. L., Rose, V., and De Gutiérrez, R. M. (2011). Evolution of binder structure in sodium silicate-activated slag-metakaolin blends. *Cem. Concr. Compos.* 33 (1), 46–54. doi:10.1016/j.cemconcomp.2010.09.004

Bílek Jr, V., Švec, J., Másilko, J., and Kalina, L. (2024). Comparison of thermogravimetry response of alkali-activated slag and Portland cement pastes after stopping their hydration using solvent exchange method. *J. Therm. Anal. Calorim.* 147 (1), 1–25. doi:10.1007/s10973-024-12934-5

Bilim, C., and Atiş, C. D. (2012). Alkali activation of mortars containing different replacement levels of ground granulated blast furnace slag. *Constr. Build. Mater.* 28 (1), 708–712. doi:10.1016/j.conbuildmat.2011.10.018

Cai, X., Cao, Z., Sun, J., Zhang, Y., and Wu, S. (2024). Influence of steel slag on properties of cement-based materials: a review. *Buildings* 14 (9), 2985. doi:10.3390/buildings14092985

Dai, J., Wang, Q., Lou, X., Bao, X., Zhang, B., Wang, J., et al. (2021). Solution calorimetry to assess effects of water-cement ratio and low temperature on hydration heat of cement. *Constr. Build. Mater.* 269, 121222. doi:10.1016/j.conbuildmat.2020.121222

Ding, X., Du, H., Wu, E., Li, Z., Li, Y., Luo, Y., et al. (2024). Investigating the hydration, mechanical properties, and pozzolanic activity of cement paste containing co-combustion fly ash. *Buildings* 14 (5), 1305. doi:10.3390/buildings14051305

Escalante-Garcia, J. I. (2003). Nonevaporable water from neat OPC and replacement materials in composite cements hydrated at different temperatures. *Cem. Concr. Res.* 33 (11), 1883–1888. doi:10.1016/s0008-8846(03)00208-4

Fang, F., Wang, Z., Zhang, F., Li, D., Jia, Z., Wang, Z., et al. (2024). Experimental study of alkali-excited steel slag–granulated blast furnace slag–cement-based grouting material based on response surface methodology. *Buildings* 14 (12), 3841. doi:10.3390/buildings14123841

Fang, G., Ho, W. K., Tu, W., and Zhang, M. (2018). Workability and mechanical properties of alkali-activated fly ash-slag concrete cured at ambient temperature. *Constr. Build. Mater.* 172, 476–487. doi:10.1016/j.conbuildmat.2018.04.008

Fang, K., Wang, D., and Gu, Y. (2023). Utilization of gasification coarse slag powder as cement partial replacement: hydration kinetics characteristics, microstructure and hardening properties. *Materials* 16 (5), 1922. doi:10.3390/ma16051922

Gao, X., Yu, Q. L., and Brouwers, H. J. H. (2015). Reaction kinetics, gel character and strength of ambient temperature cured alkali activated slag–fly ash blends. *Constr. Build. Mater.* 80, 105–115. doi:10.1016/j.conbuildmat.2015.01.065

García-Lodeiro, I., Palomo, A., Fernández-Jiménez, A., and Macphee, D. E. (2011). Compatibility studies between NASH and CASH gels. Study in the ternary diagram $Na_2O$–CaO–$Al_2O_3$–$SiO_2$–$H_2O$. *Cem. Concr. Res.* 41 (9), 923–931. doi:10.1016/j.cemconres.2011.05.006

Gholizadeh-Vayghan, A., Meza Hernandez, G., Kingne, F. K., Zhang, Y., Dilissen, N., El Kadi, M., et al. (2024). Thermal reactivation of hydrated cement paste: properties and impact on cement hydration. *Materials* 17 (11), 2659. doi:10.3390/ma17112659

Ghorbani, S., Stefanini, L., Sun, Y., Walkley, B., Provis, J. L., De Schutter, G., et al. (2023). Characterisation of alkali-activated stainless steel slag and blast-furnace slag cements. *Cem. Concr. Compo* 143, 105230. doi:10.1016/j.cemconcomp.2023.105230

Guan, J., Zhang, Y., Yao, X., Li, X., Zhang, L., and Yi, J. (2021). Experimental study on the effect of compound activator on the mechanical properties of steel slag cement mortar. *Crystals* 11 (6), 658. doi:10.3390/cryst11060658

Guo, J., Bao, Y., and Wang, M. (2018a). Steel slag in China: treatment, recycling, and management. *Waste Manage.* 78, 318–330. doi:10.1016/j.wasman.2018.04.045

Guo, Y., Xie, J., Zheng, W., and Li, J. (2018b). Effects of steel slag as fine aggregate on static and impact behaviours of concrete. *Constr. Build. Mater.* 192, 194–201. doi:10.1016/j.conbuildmat.2018.10.129

He, R., and Lu, N. L. (2023). Unveiling the dielectric property change of concrete during hardening process by ground penetrating radar with the antenna frequency of 1.6 GHz and 2.6 GHz. *Cem. Concr. Compos.* 144, 105279. doi:10.1016/j.cemconcomp.2023.105279

He, R., Nantung, T., and Lu, N. L. (2024). Unraveling microstructural evolution in air-entrained mortar and paste: insights from MIP and micro-CT tomography amid cyclic freezing-thawing damage. *J. Build. Eng.* 94, 109922. doi:10.1016/j.jobe.2024.109922

He, R., Nantung, T., Olek, J., and Lu, N. (2023). Field study of the dielectric constant of concrete: a parameter less sensitive to environmental variations than electrical resistivity. *J. Build. Eng.* 74, 106938. doi:10.1016/j.jobe.2023.106938

Huang, H., Huang, T., Yuan, Q., Zhou, D., Deng, D., and Zhang, L. (2019). Temperature dependence of structural build-up and its relation with hydration kinetics of cement paste. *Constr. Build. Mater.* 201, 553–562. doi:10.1016/j.conbuildmat.2018.12.226

Ji, Q., Wang, Y., Jia, X., Liu, Z., Zhang, J., Chen, P., et al. (2024). Study on impact resistance of alkali-activated slag cementitious material with steel fiber. *Buildings* 14 (11), 3442. doi:10.3390/buildings14113442

Ji, X., Wang, X., Zhao, X., Liu, Y., Zhang, H., and Liu, J. (2023). Properties, microstructure development and life cycle assessment of alkali-activated materials containing steel slag under different alkali equivalents. *Materials* 17 (1), 48. doi:10.3390/ma17010048

Jing, W., Jiang, J., Ding, S., and Wang, Y. (2020). Hydration and microstructure of steel slag as cementitious material and fine aggregate in mortar. *Molecules* 25 (19), 4456. doi:10.3390/molecules25194456

Joseph, S., and Cizer, Ö. (2022). Hydration of hybrid cements at low temperatures: a study on portland cement-blast furnace slag—$Na_2SO_4$. *Materials* 15 (5), 1914. doi:10.3390/ma15051914

Kua, H. W. (2015). Integrated policies to promote sustainable use of steel slag for construction—a consequential life cycle embodied energy and greenhouse gas emission perspective. *Energy Build.* 101, 133–143. doi:10.1016/j.enbuild.2015.04.036

Li, B., Lu, X., Huo, B., Zhang, Y., Liu, Y., Cheng, Y., et al. (2023). The early age hydration products and mechanical properties of cement paste with steel

slag powder as additive under steam curing conditions. *Buildings* 13 (9), 2192. doi:10.3390/buildings13092192

Li, J., Yu, Q., Wei, J., and Zhang, T. (2011). Structural characteristics and hydration kinetics of modified steel slag. *Cem. Concr. Res.* 41 (3), 324–329. doi:10.1016/j.cemconres.2010.11.018

Li, L., Feng, T., Li, Y., Zhang, Y., Sun, W., and Liu, Z. (2024). Evaluating the effect of high fly ash content and low curing temperature on early hydration heat of blended cement based on isothermal calorimetric method. *Constr. Build. Mater.* 430, 136110. doi:10.1016/j.conbuildmat.2024.136110

Liu, J., Li, Y., Ouyang, P., and Yang, Y. (2015). Hydration of the silica fume-Portland cement binary system at lower temperature. *Constr. Build. Mater.* 93, 919–925. doi:10.1016/j.conbuildmat.2015.05.056

Liu, J., Liu, B., Ge, X., Chen, Y., Song, G., Liu, K., et al. (2024). Analysis of hydration mechanism of steel slag-based cementitious materials under saline–alkaline-coupled excitation. *Buildings* 14 (3), 597. doi:10.3390/buildings14030597

Liu, P., Chen, G., Liu, G., Liu, H., Zhang, J., Chen, P., et al. (2024). Study on impact resistance of alkali-activated slag cementitious material with steel fiber. *Buildings* 14 (11), 3442. doi:10.3390/buildings14113442

Liu, P., Zhong, J., Zhang, M., Mo, L., and Deng, M. (2021). Effect of CO2 treatment on the microstructure and properties of steel slag supplementary cementitous materials. *Constr. Build. Mater.* 309, 125171. doi:10.1016/j.conbuildmat.2021.125171

Liu, W., Li, H., Zhu, H., and Xu, P. (2020). Effects of steel-slag components on interfacial-reaction characteristics of permeable steel-slag–bitumen mixture. *Materials* 13 (17), 3885. doi:10.3390/ma13173885

Liu, Z., Zhang, D. W., Li, L. I., Wang, J. X., Shao, N. N., and Wang, D. M. (2019). Microstructure and phase evolution of alkali-activated steel slag during early age. *Constr. Build. Mater.* 204, 158–165. doi:10.1016/j.conbuildmat.2019.01.213

Ma, B., Zhang, T., Tan, H., Liu, X., Mei, J., Qi, H., et al. (2018). Effect of triisopropanolamine on compressive strength and hydration of cement-fly ash paste. *Constr. Build. Mater.* 179, 89–99. doi:10.1016/j.conbuildmat.2018.05.117

Mai, H. H., Phan, D. H., and Nguyen, D. L. (2020). Responses of concrete using steel slag as coarse aggregate replacement under splitting and flexure. *Sustainability* 12 (12), 4913–4924. doi:10.3390/su12124913

Marvila, M. T., Azevedo, A. R. G. D., and Vieira, C. M. F. (2021). Reaction mechanisms of alkali-activated materials. *Ibracon Estrut. Mater.* 14, e14309. doi:10.1590/s1983-41952021000300009

Miah, M. J., Patoary, M. M. H., Paul, S. C., Babafemi, A. J., and Panda, B. (2020). Enhancement of mechanical properties and porosity of concrete using steel slag coarse aggregate. *Materials* 13 (12), 2865. doi:10.3390/ma13122865

Monshi, A., and Asgarani, M. K. (1999). Producing Portland cement from iron and steel slags and limestone. *Cem. Concr. Res.* 29 (9), 1373–1377. doi:10.1016/s0008-8846(99)00028-9

Moon, H., Ramanathan, S., Suraneni, P., Weiss, J., Lee, C. J., and Chung, C. W. (2018). Revisiting the effect of slag in reducing heat of hydration in concrete in comparison to other supplementary cementitious materials. *Materials* 11 (10), 1847. doi:10.3390/ma11101847

Myers, R. J., Bernal, S. A., San Nicolas, R., and Provis, J. L. (2013). Generalized structural description of calcium–sodium aluminosilicate hydrate gels: the cross-linked substituted to bermorite model. *Langmuir* 29 (17), 5294–5306. doi:10.1021/la4000473

Parron-Rubio, M. E., Perez-García, F., Gonzalez-Herrera, A., and Rubio-Cintas, M. D. (2018). Concrete properties comparison when substituting a 25% cement with slag from different provenances. *Materials* 11 (6), 1029. doi:10.3390/ma11061029

Provis, J. L. (2014). "Alkali activated materials," in *RILEM state-of-the-art reports*. Editors J. L. Provis, and J. S. J. van Deventer (Berlin, Germany: Springer).

Provis, J. L., and Bernal, S. A. (2014). Geopolymers and related alkali-activated materials. *Annu. Rev. Mater. Res.* 44 (1), 299–327. doi:10.1146/annurev-matsci-070813-113515

Provis, J. L., Palomo, A., and Shi, C. (2015). Advances in understanding alkali-activated materials. *Cem. Concr. Res.* 78, 110–125. doi:10.1016/j.cemconres.2015.04.013

Qasrawi, H., Shalabi, F., and Asi, I. (2009). Use of low CaO unprocessed steel slag in concrete as fine aggregate. *Constr. Build. Mater.* 23 (2), 1118–1125. doi:10.1016/j.conbuildmat.2008.06.003

Ren, P., Zhang, W., Ye, X., and Li, J. (2024). Mechanical properties and constitutive model of geopolymer lightweight aggregate concrete. *Buildings* 15 (1), 98. doi:10.3390/buildings15010098

Richardson, I. G. (2008). The calcium silicate hydrates. *Cem. Concr. Res.* 38 (2), 137–158. doi:10.1016/j.cemconres.2007.11.005

Sengupta, J., Dhang, N., and Deb, A. (2024). A cost-effective slag-based mix activated with soda ash and hydrated lime: a pilot study. *Pract. Period. Struct.* 29 (2), 04024003. doi:10.1061/ppscfx.sceng-1426

Shen, W., Liu, Y., Wu, M., Zhang, D., Du, X., Zhao, D., et al. (2020). Ecological carbonated steel slag pervious concrete prepared as a key material of sponge city. *J. Clean. Prod.* 256, 120244. doi:10.1016/j.jclepro.2020.120244

Sheng, G., Li, C., Jin, S., and Zhang, Y. (2023). Effects of steel slag powder as a cementitious material on compressive strength of cement-based composite. *Minerals* 13 (7), 869. doi:10.3390/min13070869

Shi, C., and Fernández-Jiménez, A. (2006). Stabilization/solidification of hazardous and radioactive wastes with alkali-activated cements. *J. Hazard. Mater.* 137 (3), 1656–1663. doi:10.1016/j.jhazmat.2006.05.008

Shi, C., Jiménez, A. F., and Palomo, A. (2011). New cements for the 21st century: the pursuit of an alternative to Portland cement. *Cem. Concr. Res.* 41 (7), 750–763. doi:10.1016/j.cemconres.2011.03.016

Shi, C., Roy, D., and Krivenko, P. (2003). *Alkali-activated cements and concretes*. 1st Edn. London, United Kingdom: CRC Press.

Singh, S. K., and Vashistha, P. (2021). Development of newer composite cement through mechano-chemical activation of steel slag. *Constr. Build. Mater.* 268, 121147. doi:10.1016/j.conbuildmat.2020.121147

Song, Q., He, Q., Nie, J., Wang, T., Zhou, H., Hu, Y., et al. (2024). The properties of magnesium silicate hydrate prepared from the magnesium silicate minerals in the Earth's crust. *Buildings* 14 (5), 1188. doi:10.3390/buildings14051188

Standardization Administration of China (2005). *GB/T 12957-2005: test method for activity of industrial waste slag used as addition to cement*. Beijing: China Standards Press.

Standardization Administration of China (2007). *GB 175-2007: common Portland cement*. Beijing, China: China Standards Press.

Standardization Administration of China (2011). *GB/T 1346-2011: test methods for water requirement of normal consistency, setting time and soundness of the Portland cement*. Beijing: China Standards Press.

Stepkowska, E., Aviles, M., Blanes, J., and García, R. (2007). Gradual transformation of $Ca(OH)_2$ into $CaCO_3$ on cement hydration: XRD study. *J. Therm. Anal. Calorim.* 87 (1), 189–198. doi:10.1007/s10973-006-7840-7

Sun, J., Zhang, Z., Zhuang, S., and He, W. (2020). Hydration properties and microstructure characteristics of alkali-activated steel slag. *Constr. Build. Mater.* 241, 118141. doi:10.1016/j.conbuildmat.2020.118141

Usherov-Marshak, A., Vaičiukynienė, D., Krivenko, P., and Zhang, Y. (2021). Calorimetric studies of alkali-activated blast-furnace slag cements at early hydration processes in the temperature range of 20–80° C. *Materials* 14 (19), 5872. doi:10.3390/ma14195872

Verre, S. (2021). Effect of different environments' conditioning on the debonding phenomenon in fiber-reinforced cementitious matrix-concrete joints. *Materials* 14 (24), 7566. doi:10.3390/ma14247566

Wang, H., Gu, X., Xu, X., Zhao, L., Zhu, Z., and Wang, S. (2024). Effect of diethanol-isopropanolamine and typical supplementary cementitious materials on the hydration mechanism of BOF slag cement pastes. *Buildings* 14 (5), 1268. doi:10.3390/buildings14051268

Wang, M., Xu, J., Zhang, X., Li, H., and Mei, Y. (2024). Mechanical performance optimization and microstructural mechanism study of alkali-activated steel slag–slag cementitious materials. *Buildings* 14 (5), 1204. doi:10.3390/buildings14051204

Wei, X., Sun, X., Du, H., Zhang, Y., Kong, X., and Ren, C. (2024). Recycle of steel slag as cementitious material and fine aggregate in concrete: mechanical, durability property and environmental impact. *Environ. Sci. Pollut. R.* 31 (44), 56194–56209. doi:10.1007/s11356-024-34746-0

Xiong, Z., Lin, L., Qiao, S., Li, L., Li, Y., He, S., et al. (2022). Axial performance of seawater sea-sand concrete columns reinforced with basalt fibre-reinforced polymer bars under concentric compressive load. *J. Build. Eng.* 47, 103828. doi:10.1016/j.jobe.2021.103828

Xue, Y., Wu, S., Hou, H., and Zha, J. (2006). Experimental investigation of basic oxygen furnace slag used as aggregate in asphalt mixture. *J. Hazard. Mater* 138 (2), 261–268. doi:10.1016/j.jhazmat.2006.02.073

Yang, J., Liu, L., Zhang, G., Li, H., and Sun, X. (2023). The preparation of ground blast furnace slag-steel slag pavement concrete using different activators and its performance investigation. *Buildings* 13 (7), 1590. doi:10.3390/buildings13071590

Yi, H., Xu, G., Cheng, H., Wang, J., Wan, Y., and Chen, H. (2012). An overview of utilization of steel slag. *Procedia Environ. Sci.* 16, 791–801. doi:10.1016/j.proenv.2012.10.108

You, N., Li, B., Cao, R., Shi, J., and Zhang, Y. (2019). The influence of steel slag and ferronickel slag on the properties of alkali-activated slag mortar. *Constr. Build. Mater.* 227, 116614. doi:10.1016/j.conbuildmat.2019.07.340

Zhang, B., Tan, H., Shen, W., Xu, G., Ma, B., and Ji, X. (2018). Nano-silica and silica fume modified cement mortar used as surface protection material to enhance

the impermeability. *Cem. Concr. Compo* 92, 7–17. doi:10.1016/j.cemconcomp.2018.05.012

Zhang, G., Zhang, B., Hao, Y., Pang, Q., Tian, L., Ding, R., et al. (2024). Effects of lime powder on the properties of Portland cement–sulphoaluminate cement composite system at low temperature. *Materials* 17 (15), 3658. doi:10.3390/ma17153658

Zhang, Q., Ji, T., Yang, Z., Wang, C., and Wu, H. C. (2020). Influence of different activators on microstructure and strength of alkali-activated nickel slag cementitious materials. *Constr. Build. Mater.* 235, 117449. doi:10.1016/j.conbuildmat.2019.117449

Zhang, S., and Niu, D. (2023). Hydration and mechanical properties of cement-steel slag system incorporating different activators. *Constr. Build. Mater.* 363, 129981. doi:10.1016/j.conbuildmat.2022.129981

Zhang, T., Ma, B., Jiang, D., Jiang, Q., and and, Z. (2021). Comparative research on the effect of various mineral admixtures on the early hydration process of cement. *Constr. Build. Mater.* 301, 124372. doi:10.1016/j.conbuildmat.2021.124372

Zhang, Y., Zhang, S., Nie, Q., Li, J., and Wang, W. (2023). Mechanical properties and microscopic mechanism of a multi-cementitious system comprising cement, fly ash, and steel slag powder. *Materials* 16 (22), 7195. doi:10.3390/ma16227195

Zhang, Z., Wang, Q., and Yang, J. (2017). Hydration mechanisms of composite binders containing phosphorus slag at different temperatures. *Constr. Build. Mater.* 147, 720–732. doi:10.1016/j.conbuildmat.2017.04.202

Zhong, J., Cao, L., Li, M., Wang, Y., Liu, F., Lv, X. w., et al. (2023). Mechanical properties and durability of alkali-activated steel slag–blastfurnace slag cement. *J. Iron Steel Res. Int.* 30 (7), 1342–1355. doi:10.1007/s42243-023-01003-6

Zhou, L., Chen, P., Hu, C., Zhang, Y., and Liang, Z. (2023). Study on the mechanical properties and hydration behavior of steel slag–red mud–electrolytic manganese residue based composite mortar. *Appl. Sci-Basel.* 13 (10), 5913. doi:10.3390/app13105913

Zhuang, S., and Wang, Q. (2021). Inhibition mechanisms of steel slag on the early-age hydration of cement. *Cem. Concr. Res.* 140, 106283. doi:10.1016/j.cemconres.2020.106283